

Modeling, Control and Optimal Trajectory Determination for an Autonomous Sailboat

Carl Strömbeck



LUND
UNIVERSITY

Department of Automatic Control

MSc Thesis
TFRT-6038
ISSN 0280-5316

Department of Automatic Control
Lund University
Box 118
SE-221 00 LUND
Sweden

© 2017 by Carl Strömbeck. All rights reserved.
Printed in Sweden by Tryckeriet i E-huset
Lund 2017

Abstract

A fleet of autonomous sailboat could change our perception of the planet. An autonomous sailboat could not only conduct environmental research but also perform month long operations through the energy efficient wind propulsion. This thesis is the work behind the development of an autonomous catamaran model sailboat.

A new mathematical model is brought forward and implemented for simulations performed alongside the proposed control strategy. The model and control strategy is evaluated and empirically verified to work as a subsystem for the optimal trajectory control approach. This method for planning the trajectory of the boat and still avoiding the constraint of the wind is presented as an important step to achieve the end goal of autonomous sailing.

The experimental setup performed well, except for some turbulence induced by the wind fans installed to create the artificial wind field at the test site. Both the mathematical model and the controller cause no issues with regards to simulating the motion of the boat. An extended abstract of the paper submitted related to this thesis has been presented successfully at the International Conference on Robotics and Automation 2017 in Singapore.

Acknowledgements

I would like to use this part to initially express my appreciation to Professor Alex Huihuan Qian for inviting me to The Chinese University of Hong Kong (Shenzhen) - (CUHK(SZ)) to conduct my studies. I want to thank Professor Qian for all our discussions, your advice has been deeply appreciated.

I want to thank Zuhuan Qiao at The Chinese University of Hong Kong (Shenzhen) for all our discussions and collaborations.

I would also like to thank Professor Tore Hägglund at the Department of Automatic Control at Lund University, Faculty of Engineering. I want to thank Professor Hägglund for all his thoughts and encouraging e-mails.

Furthermore, I would also like to thank all of the staff at the Robotics and Intelligent Manufacturing Lab for your help in adopting to your Chinese culture, most extraordinary food experiences and the hard work at the lab.

Contents

List of Figures	9
List of Tables	12
1. Introduction	13
1.1 Motivation	13
1.2 Background	14
1.3 Autonomous Robotic Sailboat Project	14
1.4 Principles of Sailing	16
1.5 Description of Concepts and Units	18
1.6 Thesis Outline	21
1.7 Related Publications	22
2. Platform Description	23
2.1 Hardware Setup	24
2.2 Software Setup	25
2.3 External Aids	28
3. Modeling	30
3.1 Model	30
3.2 External Forces	35
3.3 Parameter Identification	39
4. Control	41
4.1 Heading Error	42
4.2 Control Outputs	44
5. Optimal Trajectory Control	47
5.1 Path Planning Algorithms	47
5.2 Multi-Variable Path Planning	50
5.3 Combining the Costs	58
5.4 Optimal Trajectory Control Analysis	59
5.5 Strategic Path Determination	59

Contents

6. Experiments and Simulations	62
6.1 Force Polar Diagram Experiments	62
6.2 Test Site Experiments	63
6.3 Catamaran Simulations	67
6.4 Heading Control Simulations	67
6.5 Sail Control Simulations	70
7. Conclusions	71
7.1 Conclusion	71
7.2 Future Work	72
Bibliography	73

List of Figures

1.1	Catamaran used by the Chinese University of Hong Kong, Shenzhen	15
1.2	A schematic side view of the catamaran, including the most important components.	16
1.3	Points of Sail, the different directions that one can sail in relation to the apparent wind.	17
1.4	The catamaran base frame and the notations of the different motions and directions.	19
1.5	Relationship between the real wind and the apparent wind as the boat moves forward.	20
1.6	Coordinate systems for both catamaran and inertial frame.	21
2.1	The catamaran model sailboat in the pool used for various experiments.	23
2.2	Overview of the hardware setup for the sailing platform with the hardware not included on the boat communicating via Bluetooth.	24
2.3	Experimental pool setup with external aids for artificial wind field.	26
2.4	Explanatory tacking trajectory in pool.	27
2.5	The state machine and transitions between different states.	27
2.6	Schematic view of the simulation environment and the functions underlying it.	28
2.7	Electronic components on and off the catamaran. Left: Development Board [Arduino Bluno, 2017]. Middle: OPTO Force Sensor [OMD-20-FG-100N DATASHEET, 2017]. Right: Vaavud Wind Sensor [Vaavud Sleipnir, 2017].	29
3.1	The catamaran model sailboat with the input parameters used for mathematical modeling	32
3.2	The catamaran model sailboat with focus on the dagger board foils mounted on the bottom of the hull to reduce drift	33

List of Figures

3.3	The mast and sails are attached in the hole of this 3D-printed part is printed using an Ultimaker 2+. One can attach the OPTO force sensor underneath this hole and use this to sense the wind.	36
3.4	F_x and F_y forces in the sail frame display.	37
3.5	An example scenario of how the controlled sail angle can differ from the real sail angle. The red sail is the controlled sail and the green is the real. The dotted line is the directional center line of the boat with the upward direction towards the bow.	38
3.6	A Velocity Polar Diagram for an arbitrary sailboat. The curves display the velocity made good of a boat at different wind conditions. This is commonly used for determining what heading one should set to reach a position as fast as possible. The fastest downwind heading is shown by the red dots.	39
4.1	Example scenario of how a wind shift can impact an incorrect heading angle. State 1: Wind from right, red trajectory heading straight towards the target position and green trajectory heading slightly higher towards the wind. State 2: Wind shift to left, red trajectory needs to perform two tacks to complete the mission of reaching the mark and green trajectory reaches the target without making any major maneuvers.	43
4.2	How the Course over Ground is affected by the drift velocity. The real heading is the sum of θ and θ_{drift}	43
5.1	Plot of the wind field in the pool used for experiments. To aid use of the potential field method favoring places with higher wind speeds.	49
5.2	ASV Roboat, developed by Austrian Society for Innovative Computer Sciences which uses the Velocity Polar Diagram for planning it's path	50
5.3	Figure showing the different angles and heading errors. for the catamaran sailing towards a target.	51
5.4	Graph of the Target Cost, x-axis is the e_{Target} and y-axis is the cost . . .	52
5.5	Graph of the VPD Cost, the boat speed is in relation to the wind angle	53
5.6	Graph of the Obstacles, the boat is located at the origin and the bearings of the obstacles are shown in the figure. These obstacles are related to the costs shown in Figure 5.7.	54
5.7	Graph of the Obstacle Cost, x-axis is the bearing towards the obstacle and y-axis is the cost based on a fictional configuration of obstacles shown in Figure 5.4	54
5.8	Graph of the Action Cost, x-axis is the heading change and y-axis is the cost.	55
5.9	Graph of the right-of-way part of the Strategic Cost, x-axis is the Apparent Wind and y-axis is the cost.	56

5.10 This figure show two different paths for the boat advancing towards the top mark. the wind is initially coming more from the left and then after position two it turns. The green boat tacks before the layline and still reach the mark, sailing a shorter path. The second boat does not favor sailing closer to the center and tacks later.	57
5.11 Graph of the Wave Cost, x-axis is the Apparent Wind and y-axis is the cost.	58
5.12 Graph of example scenario with the target position located at the top forcing the boat to sail upwind to reach the target position, the different dotted lines are potential paths to be determined by the optimal trajectory control	60
5.13 Graph of example scenario with the obstacle cost highlighted.	60
5.14 Graph of example scenario with the action cost highlighted.	61
5.15 Graph of example scenario with the target cost highlighted.	61
5.16 Graph of example scenario and the combined total cost assigned to the current situation	61
 6.1 The experimental setup of extracting the forces generated by the wind.	63
6.2 The apparent wind angle is ψ and measurements are made at every other angle with the angles 90° to 270° mirrored to the remaining 180° .	64
6.3 The Force Polar Diagram with the F_x force plotted with reference to the apparent wind angle. This is at the wind speed of 2 m/s.	64
6.4 The Force Polar Diagram with the F_x force plotted with reference to the apparent wind angle. This is at the wind speed of 2 m/s.	65
6.5 The Force Diagram with the y-force plotted with reference to the apparent wind angle. This is at the wind speed of 2 m/s. With different configurations, with $0 \leq \theta \leq 90$	65
6.6 Boat speed using the Force Polar Diagram to set the sail angle versus the predefined sail angle.	66
6.7 This figure show the different relations between the optimal trajectory control level, control and dynamics.	68
6.8 Simulation of the boat sailing upwind. the controller receives pulses of desired headings and is controlled thereafter, the wind is going at a 180° θ angle.	69
6.9 Boat speed(yellow) and drift speed(blue) with different simulated sail angles in a ramp function.	70

List of Tables

2.1	Specifications of Joysway BINARY	25
3.1	Non Experimental Parameters. Parameters not determined through tests or simulations.	40
4.1	Non Experimental Parameters. Parameters not determined through tests or simulations.	45
6.1	Experimental Parameters. Parameters determined through tests and simulations.	69

1

Introduction

The art of sailing dates back to thousands of years. The methods have been widely developed since then and over this time an essential part to both fishing and trade. There is of course maybe the most important field of use, exploration, without this method of sailing it might be possible that many of the locations on our planet would be discovered much later.

Sailing also holds one of the oldest and most prestigious sporting events known, the America's Cup. Sailing is still used for fishing in less developed parts of the world and works perfectly as a means of transportation. On more industrialized locations of the world it is now merely used as an activity and for sporting events, but is still an important means of transportation as it requires no or low energy.

It is common to have an autopilot installed on any kind of conventional sailboat destined for anything but competing. Most of these autopilots struggle when the sea conditions get rough and when the wind is too strong. These conditions create an unstable control, especially for the boats heading. The fully autonomous operations of commercial sailboats are today highly limited.

1.1 Motivation

Autonomous sailing is in essence not new. The nautical world's cargo ships use autopilot when at sea and even small sailboats often have autopilot installed controlling the heading angle. It has been like this for the past couple of decades without any extreme progress in the commercial world. The commercial autopilots for sailboats are normally not equipped with the essential mechanics or software to operate fully autonomously with reference to the wind, currents, waves or destinations.

Numerous research projects have been carried out for the past years, all with the purpose of mastering the art of autonomous sailing. This area of research has also reached the commercial market where e.g. Saildrone inc.¹ in Alameda, USA develops autonomous sailboats and use them for collecting environmental data. While

¹ www.saildrone.com

there are dozens of companies just in San Francisco that develop autonomous cars, Saildrone actually already commercialized their boat and turned it into a business, selling the data that the sailing drones collect.

One of the most important purposes for conducting this research is the fact that a solution that uses the wind as a propelling force is far more energy efficient than vessels propelled with fossil fuels. This technique could also decrease the cost of research and increase the knowledge of our planet, simultaneously. The goal is to improve the knowledge within the field of autonomous sailing that in itself can impact the way we look at our oceans today.

1.2 Background

Understanding the oceans are of great importance since our planet is largely covered by water. To better understand how our actions impact the planet collecting high quality data is important. As of now multiple methods for collecting this data exist, the most dynamic method is using a research ship, but this might also be the most expensive method. There are sub-surface moorings attached to the bottom of the ocean and collect data at a certain depth. Satellite tracked surface drifters are also used among many other solutions.

Research ships are the most expensive method and the cost of using such a research vessel is high, these manned research ships can cost between \$US20,000 and \$US50,000 per day [Kaiser, 2011]. This can be decreased significantly through the use of unmanned ships. One important cost driving factor is the danger that the researchers put themselves through, a cost that can be eliminated completely with an autonomous sailboat. Saildrone charges \$US2,500 for one day of data collection in the area of the customers interests, it might not be able to collect all the data that a research ship can, but close, the data that it can collect is at a fraction of the cost of a research ship.

1.3 Autonomous Robotic Sailboat Project

The Chinese University of Hong Kong, Shenzhen initiated the Autonomous Robotic Sailboat project during the fall of 2016. A project that is partially supported by the State Joint Engineering Lab and Shenzhen Engineering Lab on Robotics and Intelligent Manufacturing, Shenzhen, China.

The project aims to contribute to the novel art of autonomous sailing. It has the initial goal of achieving autonomous sailing on a small model sailboat and the future goal of implementing these discoveries on a full-scale boat for offshore sailing. One of the purposes of the project is to create awareness about environmental ways for ocean transportation and oceanic data collection. The project will be performed by the Robotics and Intelligent Manufacturing Lab through a series of studies, also known as Robotics and Artificial Intelligence Lab (RAIL).



Figure 1.1 Catamaran used by the Chinese University of Hong Kong, Shenzhen

The initial platform used is a catamaran model sailboat, shown in Figure 1.1. One of the future platforms that are to be used is a mini 12² sailboat, used in the Microtransat Challenge presented in Section 1.3.

Competitions and Conferences

The field of research has become more known over the past decade. A few initiatives have been taken to highlight this field of research. Two of the most famous initiatives are presented in this section. An event that is not presented here is the Sailbot³ event taking place in North America for students.

World Robotic Sailing Championship/International Robotic Sailing Conference
 Starting in 2008, a yearly conference is held to encourage research projects in the field of robotic sailing. The Robotic Sailing Conference is held together with the World Robotic Sailing Championship⁴. It is a gathering where different research teams come together to share their experiences and compete for the championship. One milestone for the project by CUHK(SZ) is to participate in this competition.

Microtransat Challenge The Microtransat Challenge⁵ is a transatlantic race for autonomous boats. This is much like the World Robotic Sailing Championship an initiative to stimulate the development of autonomous sailboats through a friendly competition. This event has been taking place since 2006 but the first competition was first held in 2010. The World Robotic Sailing Championship is actually a spin-off from this event. It is in this competition the mini 12 sailboat is to be used.

² The ILLUSION Mini 12 sailboat is a small 12 feet long boat, that is controlled single handed, with foot pedals and is a common sail racing boat.

³ <http://www.sailbot.org/>

⁴ <http://www.roboticsailing.org/>

⁵ <http://www.microtransat.org/>

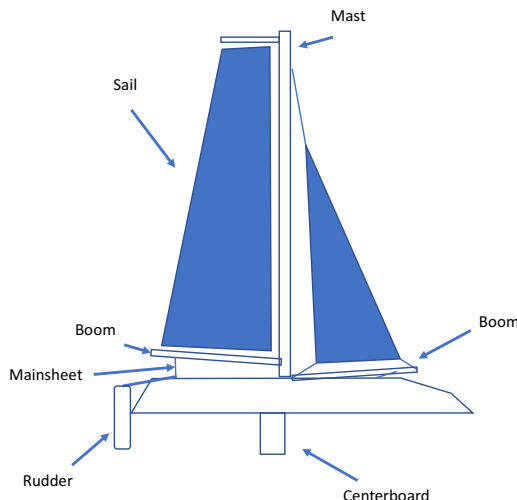


Figure 1.2 A schematic side view of the catamaran, including the most important components.

1.4 Principles of Sailing

This section describes the art of sailing, nomenclature and expressions used in other chapters. The idea of this part is to enhance the understanding of the remaining explanations.

Sailing Expressions

The different parts of the boat and sailing expressions are explained first, a catamaran (two hulls), see Figure 1.1 is used in this project but the basics are the same as a normal mono-hulled sailboat. A side-view of the catamaran can be seen in Figure 1.2, this looks similar to a mono-hulled boat and in fact much is. There are just a few things that differ e.g. the number of hulls, rudders and centerboards but mainly boat dynamics.

At the rear end of the boat, the so called stern one can see the rudders. The rudders are like thin foils and are used for controlling the yaw of the boat. The centerboards are located at the middle of the boat and are also like thin foils and are meant to minimize a swaying motion. There are two sails, one mainsail and one jib located at the front of the boat or the so called bow. To control the sail one uses sheets, these are called mainsheet and jibsheet and attaches to the hulls of the boat and the boom. The sails are attached to the mast and the boom that is attached to the mast.

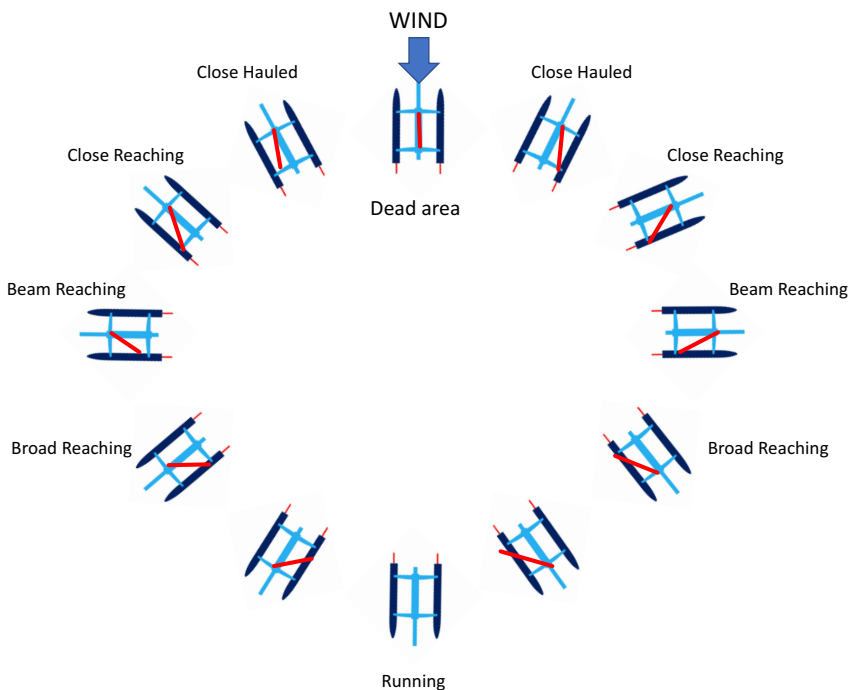


Figure 1.3 Points of Sail, the different directions that one can sail in relation to the apparent wind.

Point of Sail

It is important to know what directions a sailboat can sail in relation to the wind as the motion of the sailboat is strongly constrained to the wind as the only propelling force. In Figure 1.3 the different points of sail are shown, meaning the directions and their names.

The directions on the right hand side of the figure are directions that involves sailing on Port tack and the left hand side are the directions sailing on Starboard tack. Because of the dynamics of the boat one can not transport themselves in the directions between port's close hauled and starboard's close hauled. Sailing in the dead area will result in the coming to a complete rest. Sailing straight or close to straight downwind, away from the wind, will also not be favorable because of boat dynamics but this will still result in going downwind but not as fast as broad reaching. As one might guess going in the opposite direction is called upwind sailing.

Some additional terms used are the helmsman, the person steering the boat, the tactician, responsible for tactics and the strategist, responsible for the strategy on the boat.

Maneuvers

There are two different names explaining the change of direction. When one is turning and passing the dead area before heading the other direction, then one performs a tack and this maneuver is called tacking. The opposite directional change when heading away from the wind is called jibe or gybe.

1.5 Description of Concepts and Units

The different coordinate systems, concepts, variables and units are explained in this section. This is an attempt to explain the different reference frames and angles later used in simulations, modeling, control and trajectory control.

Coordinate systems

In order to fully describe the motions of the boat a system of reference is to be chosen. To describe the sailboat motion a coordinate system is created, fixed to the body frame of the boat. The other values are in reference to the World-reference frame if nothing else is stated.

World Frame The pose of the sailboat is normally referred to the world frame. The world frame is in the North-East-Down reference and θ is the angle around the z-axis, starting with 0° on the x-axis. This is the inertial frame and all can be referred back to the world frame. It is shown as part of Figure 1.6 as the catamaran is placed in it. The reason why this is chosen as an inertial frame is that it is a common reference frame in the nautical world, and used by many including [Fossen, 2002].

Catamaran Frame This is another important coordinate frame that has an origin at the Center of Mass of the boat. It is shown in Figure 1.4 and is used as the base frame for the sail angle and the rudder angle. This frame is also the basis of many of the equations behind the mathematical model developed in Chapter 3.

Sail Frame The sail frame might be the most important one as it is in this frame one decides what wind forces affect the boat. The sail frame is shown in Figure 3.5 and it is with this frame that the sail apparent wind angles are referred to.

Camera Frame This coordinate frame is most commonly referred to in Chapter 6. It is used for experiments as the boat is localized using a camera and therefore the position of it needs to be translated from this camera frame to the inertial world frame. The translation is rather simple as the camera is located right above the test location and the motion of the boat is assumed to be planar, same as the water.

Force Sensor Frame The force sensor is presented later in Chapter 3 and is used to determine the forces acting on the boat from the wind through the sails. This is can easily be translated as the z-axes of the boat and the sensor are parallel and the sensor is just rotated about the x-axis 180° and then 90° around the z-axis, this rotation is shown in the rotation matrix in Equation 1.1.

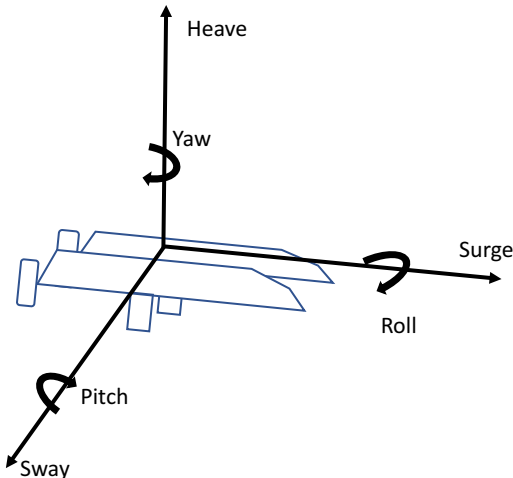


Figure 1.4 The catamaran base frame and the notations of the different motions and directions.

$$ROT_x(180)ROT_z(90) = \begin{bmatrix} 1 & 0 & 0 \\ 0 & -1 & 0 \\ 0 & 0 & -1 \end{bmatrix} \begin{bmatrix} 0 & -1 & 0 \\ 1 & 0 & 0 \\ 0 & 0 & 1 \end{bmatrix} = \begin{bmatrix} 0 & -1 & 0 \\ -1 & 0 & 0 \\ 0 & 0 & -1 \end{bmatrix} \quad (1.1)$$

Real and Apparent Wind

This concept of real and apparent wind is an important part of sailing as it is related to the wind, what as already mentioned is the most important part. The wind that appears on the boat is often not the same as the real wind as the boat moves forward, rotates and drifts. The real wind is shown in Figure 1.5 and the apparent wind is a result of the real wind which is in reference to the world frame. The relation between the two can be seen in Figure 1.5 and is caused due to the induced wind from the boat speed.

This is calculated to later be used in the mathematical model. First, the real wind is translated to translation instead of speed and direction, this is done using Equation 1.2, the variables are also shown in Figure 1.6.

$$\begin{cases} \delta_{w,x} = v_w \cos \gamma_w \\ \delta_{w,y} = v_w \sin \gamma_w \end{cases} \quad (1.2)$$

The translation of the boat is already determined in the modeling part and are referred to as \dot{x} , \dot{y} and θ . With this one can use Equation 1.3 to calculate the apparent wind speed and angle.

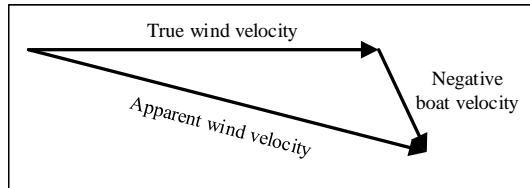


Figure 1.5 Relationship between the real wind and the apparent wind as the boat moves forward.

$$\begin{cases} v_{w,\text{apparent}} = \sqrt{\delta_{w,\text{apparent},x}^2 + \delta_{w,\text{apparent},y}^2} \\ \psi_{w,\text{apparent},\text{world}} = \arctan \frac{\delta_{w,\text{apparent},y}}{\delta_{w,\text{apparent},x}} \end{cases} \Leftarrow \begin{cases} \delta_{w,\text{apparent},x} = \delta_{w,x} - \dot{x} \\ \delta_{w,\text{apparent},y} = \delta_{w,y} - \dot{y} \end{cases} \quad (1.3)$$

This wind angle is in the world frame, for the calculations in Chapter 3 one needs to have it in both boat frame and in sail frame. This is done using Equations 1.4 and 1.5 with θ as the heading angle shown in Figure 1.6. All variables are explained later in the State Space section of this chapter.

$$\psi_{w,\text{apparent},\text{boat}} = \psi_{w,\text{apparent},\text{world}} - \theta \quad (1.4)$$

$$\psi_{w,\text{apparent},\text{sail}} = \psi_{w,\text{apparent},\text{world}} - (\theta + 180 - \delta_s) \quad (1.5)$$

State Space

In this section the state space of the model is explained. Most of the different variables are shown in Figure 1.6 or used in Equation 3.4 and are all essential for building the mathematical model of the catamaran.

Some of the most important variables are the control inputs used for controlling the boat heading, drift and speed. The rudder control is measured in angles in the same coordinate frame as the boat coordinate frame but rotated 180° around the boat z-axis. The rudder angle is denoted as δ_r . The sail is similarly referenced to the rudder and is denoted as δ_s .

The position is referred to in the world frame and is given in x- and y-coordinates. Same goes for the heading and the variable used for the heading angle is θ . The boats movement is in the same reference frame as in Figure 1.4 and the forward motion, v is in the surge direction while v_d is the sway direction, the F_{forward} and F_{drift} forces are aligned with these. ω , the angular velocity is in the boat frame and not in the world frame therefore it is shown in the opposite direction in Figure 1.6.

One can also observe the constants C_4 and C_5 , these are the physical distances from the Center of Rotation to the center of effect of the rudder forces and the distance to the mast.

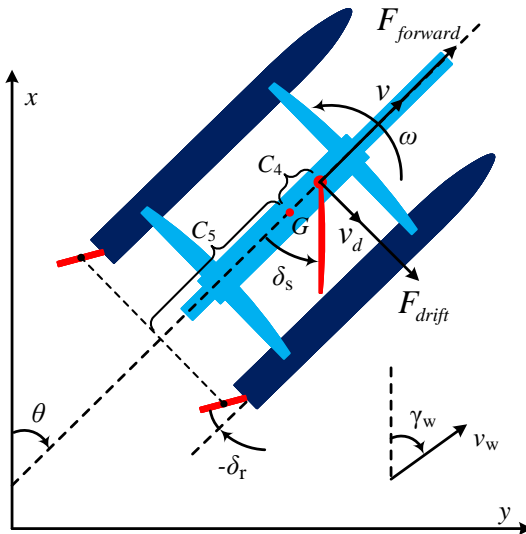


Figure 1.6 Coordinate systems for both catamaran and inertial frame.

Units and Notations

Throughout the project different notations and units are used. To start, degrees are used instead of radians as it is more common in the nautical world. The wind speed is in meters per second and not knots, $1852m/h = 1knot$ that is a nautical unit but in this case meters per second is as common. It is the same for boat speed. All measurements are made in SI units, including all calculations.

1.6 Thesis Outline

The thesis cover mathematical modeling of the catamaran model sailboat, control of it and determining an optimal path to reach a target position. A great part of the work was focused on developing and integrating the mathematical model in Matlab SIMULINK⁶. This simulation model will later be used for analysis of the algorithms used for trajectory control. This section on the other hand, focuses on the layout and the contents of each chapter the thesis covers.

Chapter 1 This chapter introduces the reader to the art of sailing, motivates the project and present the background behind it. It also covers some terms and concepts used in the project to enhance the understanding.

⁶ Simulation tool for Matlab, Matlab is a developed by MATHWORKS.

Chapter 2 This chapter goes through the catamaran thoroughly, presents the necessary aids used for experiments and analysis of the boat. It covers the different hardware components used on the boat and the basic software structure used for both experiments and for simulations.

Chapter 3 This chapter is one of the most important chapters as it captures the mathematical model of the boat. It also covers how the forces have been analyzed and then included in the model.

Chapter 4 This short chapter presents the method used for heading control as well as controlling the wind angle. The main part is about how the rudder control is approached and how it was solved.

Chapter 5 This chapter explains the complications of planning the catamaran's path from one point to another. It presents the existing work, how it has been approached in this project and the method used.

Chapter 6 This chapter is the technical chapter that links the other rather theoretical chapters to the field tests and experiments. It explains simulation results, complications and the connection between the equations and the actual developed simulation tool.

Chapter 7 This chapter concludes the thesis with suggestions. It also discusses the techniques developed and elaborates on future work.

1.7 Related Publications

At an early stage of the work for this thesis a publication was produced. It consisted of an initial mathematical model and was submitted for publication to the International Conference on Intelligent Robots and Systems (IROS) 2017 in Vancouver, Canada. The outcome of this submission will be posted on 15th of June, 2017 and the paper, "*Tacking Control of an Autonomous Sailboat Based on Force Polar Diagram*" was co-authored with Qinbo Sun, Zuhuan Qiao and Yang Qu. It was requested that the authors would write an extended 1 page abstract upon submission. This extended abstract was accepted to be presented at The 2017 IEEE International Conference on Robotics and Automation (ICRA) in Singapore on May 29th - June 3rd. Some formulations and equations in this thesis are similar to those in the paper.

2

Platform Description

The platform that was used for this project is a miniature catamaran sailboat. A regular radio controlled (RC) model sailboat is adopted to fulfill the requirements. The selection of the boat was made so that it would be easily transported to the pool where a majority of the experiments were conducted. Another convenience with having a smaller boat when developing the sailboat is that the limited size of the pool does not constrain the boat too much. A larger autonomous sailboat will be developed later in the Autonomous Robotic Sailing Project, but for cost reasons the initial research is constrained to this smaller model sailboat. The current version of the boat is shown in Figure 2.1.



Figure 2.1 The catamaran model sailboat in the pool used for various experiments.

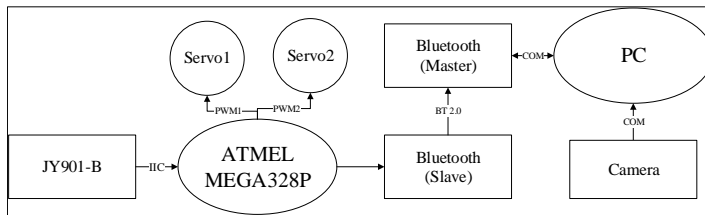


Figure 2.2 Overview of the hardware setup for the sailing platform with the hardware not included on the boat communicating via Bluetooth.

2.1 Hardware Setup

As mentioned earlier, the project was started using a RC sailboat. To this a set of electronic components was added to the boat both on the platform and externally to aid with boat localization. A set of cameras was used for localization since GPS localization is limited when it comes to accuracy in the location of the experiments, this is except for the hardware added to the conventional RC sailboat.

There are two speed controlled servo motors mounted inside the hull of the boat, one controlling the sheet which indirectly controls the sail angle and one servo controlling the two rudders and therefore the rudder angles. A JY901-B Inertial Measurement Unit (IMU) is placed inside the boat to electronically measure and report the heading of the boat. The IMU is connected to an ATMEL MEGA328P development board which controls the servos and communicates through a Bluetooth UART with the computer running the control of the boat with the help of a camera localizing the boat, this is further explained in Section 2.2. An overview of the hardware is show in Figure 2.2.

Catamaran

The catamaran platform is manufactured in Dongguan, China by Joysway and the model is a BINARY miniature catamaran [Joysway]. It has the overall length of 400 mm and consists of one mainsail and one foresail¹. Each of the two hulls has a fin also known as centerboard² and one rudder. The hulls are made of plastic and has a plastic structure that connects the two hulls and has the fiber mast connected to it. Without the extra sensors and electronic equipment the boat only weighs 360g. A photo of the boat is shown in Figure 2.1 and more specific data about the platform is shown in Table 2.1.

Electronic Components

On board the boat two servos are mounted. Both servos are located in the port hull of the boat together with a 2.4GHz 2CH receiver that controls the servos. The servos

¹ The earlier mentioned jib is a kind of small foresail

² Another word for this is daggerboard

Table 2.1 Specifications of Joysway BINARY

Parameter	Value	Entity
Length	400	mm
Beam	255	mm
Mast Height	565	mm
Total Height	710	mm
Total Weight	360	g
Jib Sail Area	2.6	dm ²
Main Sail Area	5.3	dm ²

are two 9g micro servo motors with plastic gears.

In the starboard hull one can find the ATMEL development board that is connected through a Inter-Integrated-Circuit(IIC) to a 3-axis accelerometer, a 3-axis gyroscope, a 3-axis digital compass and a barometer all included in the JY901-B IMU module. In addition to this one Bluetooth UART is connected and communicates with the computer. The development board is shown in Figure 2.7 Left.

2.2 Software Setup

The software used can be arranged and divided in different functionalities. An initial state machine setup was introduced which was used for data collection and getting to know the dynamics of the boat. This includes a localization function that imports the images from a USB connected camera facing the pool. The function extracts all pixels that has the same color code as pre-defined as existing on the boat. Through K-means clustering the boat position in the camera frame can be extracted and used in the software. The software logs all data such as rudder angle, sail angle, velocity and pose of the boat to name a few. The software also imports the data received from IMU and especially records the orientation of the boat. A view of this experimental setup is shown in Figure 2.3 where the yellow color code is used successfully.

All the data collected during these experiments are recorded and later used to develop a simulation tool which is the second part when it comes to software development for the project. The simulation tool was developed in SIMULINK with the aim to capture the dynamics of the boat without having to perform real sailing experiments. The purpose of the tool is to enhance the future development of the boat and to have a testing platform for trajectory control.

State Machine

The state machine that has been developed for the purpose of the experiments work through introducing different states in order to perform a desired sequence of maneuvers. One of the most critical maneuvers of sailing is tacking, to analyze this a 4 state control algorithm was introduced with an extra initiation state. The video

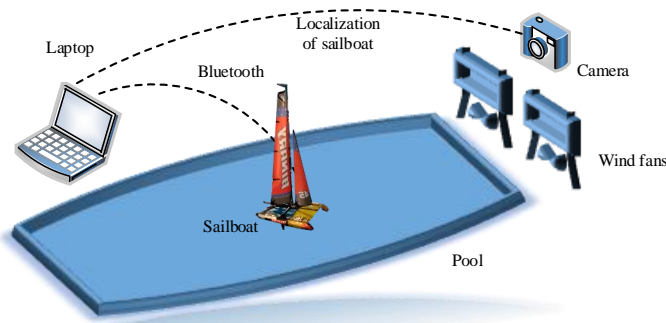


Figure 2.3 Experimental pool setup with external aids for artificial wind field.

image recorded with the camera was divided into two parts, a left part of the pool and a right part of the pool with the wind parallel to the dividing middle line, a graphical explanation of this is shown in Figure 2.4. This state machine was further developed for other maneuvers, for the tacking control the different states are shown in Figure 2.5 with the k values working as a flag to keep track of if the boat should turn right or left. This collected data from the camera was later used to calibrate the mathematical model. The following states describes how the objective of tacking is reached:

1. **Left Turning:** In this state the objective for the boat is to turn left to change direction from port to starboard. The boat ends up in this state if it is located on the Right hand side of the pool and the heading angle of the boat is in the interval $\theta \subset [33, 147]$. When in this state the rudder angle is set to $\delta_r = -25^\circ$ and the sail angle is set to $\delta_s = 5^\circ$.
2. **Right Turning:** In this state the objective for the boat is to turn right to change direction from starboard to port. The boat ends up in this state if it is located on the left hand side of the pool and the heading angle of the boat is in the interval $\theta \subset [213, 327]$. When in this state the rudder angle is set to $\delta_r = 25^\circ$ and the sail angle is set to $\delta_s = -5^\circ$.
3. **No Wind:** Since the wind field is smaller than the size of the experimental area it means that the boat can travel to an area where there is no wind. The camera covers a large part of the pool where there is wind, because of this the boat is considered to be outside the wind field if the boat can not be detected by the camera. It is then desired that the boat returns to the area with wind since the wind is the only propelling force and any movement of the boat is due to previous wind forces. If the boat can not be detected by the camera it enters this state and the control inputs are determined based on the previous state. The boat preserves the previous rudder angle and the sail is closely hauled so that any drag from the sail is minimized.

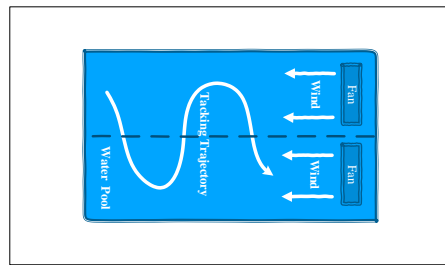


Figure 2.4 Explanatory tacking trajectory in pool.

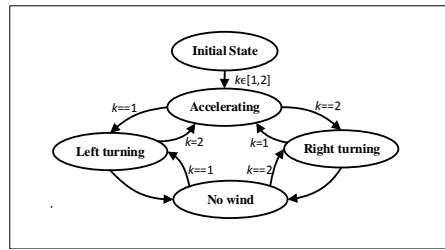


Figure 2.5 The state machine and transitions between different states.

4. **Accelerating:** If the boat does not satisfy the condition to be in any other state it ends up in this state. This means that the quest of the boat can not be fully determined and therefore the boat should focus on gaining speed so that it can translate to another state to perform one of the other maneuvers, preferably tacking. The rudder angle is set to 0° to make sure that any rudder angle is not slowing the boat down, more about the boat dynamics is explained in Chapter 3. The sail angle is set with relation to the wind direction to maximize the propelling force. It is important to notice that the boat might enter this state directly after a successful tack and this state is therefore used to gain speed again.

Simulation Environment

The simulation environment is used for developing an optimal way to control the boat as well as bring forward a higher level of path planning. This simulation environment can be structured in an hierarchical way with different levels building up from the dynamics of the boat to the highest level that consists of planning a path to reach a desired location based on all of the below levels. A simple overview of the simulation tool function and structure can be seen in Figure 2.6.

The purpose is to capture the boat dynamics and be able to experimentally bring forward the end product, meaning the trajectory control that makes sure that the boat

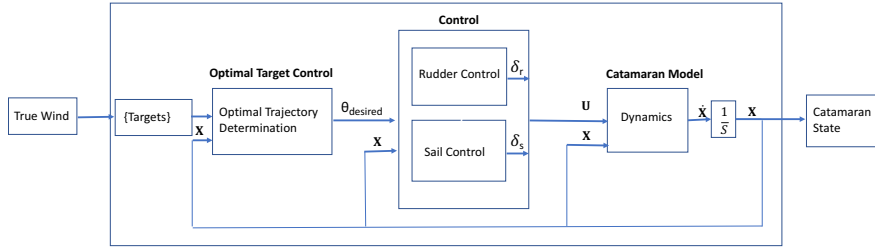


Figure 2.6 Schematic view of the simulation environment and the functions underlying it.

moves to the desired target position as fast and safe as possible. This is one of the most critical parts when it comes to sailing as it is the part that distinguishes success from failure. The different parts that the simulation environment consists of are the boat dynamics, rudder and sail control, desired heading determination and target determination. All these parts are described separately in their own Chapter and are important when it comes to achieving autonomous sailing. The dependencies and how they are all connected to each other is described in Figure 2.6.

2.3 External Aids

A set of sensors, fans, cameras and 3D-printed details were used for the development of the boat, setting up the test site and the development of the simulation environment. Since all of these have been a crucial part of the project and have effected the outcome of the work to a large extent some of the most important components will be mentioned in this part.

OPTO Force Sensor

One of the most important external aids that was used during the project was the 3D force sensor. During the studies of the wind force propelling the catamaran a force sensor was used to measure how the wind speed and direction effects the forces acting on the boat. Previous research often use the estimation that the sails can be modeled as thin foils and therefore one can calculate the forces based on the area of the sails and from that the propelling forces can be extracted. This estimation have been used by many in the past, among these [Gale and Walls, 2000] used this approach.

During the force measurements an OPTOFORCE OMD-20-FG-100N 3D force sensor was used. It has the capacity to measure 100 Newton compression and 50 Newton tension with a 6.25 mN resolution. The force sensor is shown in Figure 2.7 Middle.

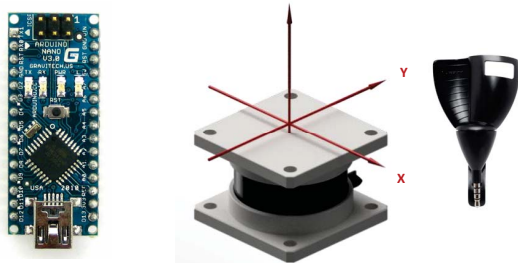


Figure 2.7 Electronic components on and off the catamaran. Left: Development Board [Arduino Bluno, 2017]. Middle: OPTO Force Sensor [OMD-20-FG-100N DATASHEET, 2017]. Right: Vaavud Wind Sensor [Vaavud Sleipnir, 2017].

Artificial Wind Field Fan

What has been discovered to be one of the most important aids during the project are the fans that create the artificial wind field during the tests. Initially all tests were performed using only two fans, but given the irregularities in the wind field that they created another fan was installed and another 4 fans has been ordered to improve the wind field even more for future work. The problems with using a small set of fans was that the wind did not only loose power just a few meters from the pool but the wind field in itself became small and any readings from how the boat was affected by the wind was hard to distinguish.

The fans that were used during the tests are designed to be used for indoor model boat sailing and each one has a 3x10m area coverage. They are all of Transit 2015 - White Horse Lake model and are shown in the background of Figure 2.1.

Vaavud Wind Sensor

There is only one propelling force when it comes to sailing, the wind. Except an occasional surf on a wave the wind constrains the boat fully, it is therefore crucial to know exactly what wind the boat is effected by. Throughout the project a wind sensor detecting both direction and wind speed was used. The Vaavud Sleipnir detects wind speeds within 2-40 m/s with 4% precision and 0.1 m/s of resolution. The Sleipnir also detects wind direction with 4% precision and is shown in Figure 2.7 Right.

3

Modeling

To study and explain the behavior of the boat a mathematical model is developed. The accuracy of the model has a great effect since this will effect the quality of most parts of this project. When it comes to modeling one can find a set of mathematical models that have previously been developed for sailboats, some of these are the ones presented by [Gale and Walls, 2000; Nuno A. Cruz, 2015; M. Tranzatto, 2015b]. The purpose of the model is mainly to explain the system behavior in order to develop an accurate controller and for the trajectory control to be as fast and safe as possible.

It is a rather complex problem one is facing when it comes to the challenge of developing an autonomous sailboat. The wind is constantly changing in both intensity and direction, the waves are extremely irregular and currents constantly change as well. It is not uncommon to simplify the mathematical model to try to capture the boat dynamics without creating a problem that is infinitely complex. A common model of reference is presented in [Xiao and Jouffroy, 2014], they reduce the movement of the boat from a 6 Degree-of-Freedom(DoF) to 4 DoF model. It is assumed that the vertical movement of the boat can be neglected, it is also assumed the the boat does not have any significant pitching motion which reduces the Degrees-of-Freedom to 4. This model has been simplified even more by neglecting the rolling motion of the boat. This was done in [Jaulin and Bars, 2013], which was used as a model of reference in this project.

3.1 Model

The mathematical model developed for the catamaran is presented in this section. The platform that has been used is a multi-hulled boat unlike many other projects developing autonomous sailboats. This means that the rolling motion of the boat is generally much less compared to a single hulled boat, due to the large base with the two hulls one can reduce the complexity of the model given the design of the boat. After running some tests with the model sailboat it was soon discovered that the rolling motion of the boat was so small it could be neglected. The magnitude

of a rolling motion on a catamaran is highly dependent of the design of the boat. Two factors that come in to play is normally the sail area and size of the boat, some simply roll more than others. In this case it is so small in the wind conditions used in the experiments and as these conditions are similar to normal wind conditions the assumption that the rolling motion is so small that it can be neglected can be assumed to be valid. With the above mentioned assumptions a 3 DoF model can be developed.

Mathematical Model

Given the above assumptions one can identify a model that describes the state of the boat and how the environment and control inputs affect this state. The catamaran description consists of the position, orientation, translation and rotation. The wind will affect the forces acting on the boat and propel the boat forward. The wind force is mainly affected by the apparent wind, the apparent wind is described in Section 1.5. Since a couple of simplifications about the dynamics of the catamaran have been made one can now develop a graspable model.

The model can be represented by the state of the boat \mathbf{X} , control inputs \mathbf{u} and the true wind \mathbf{W} . The model of the boat is described in Equation 3.1.

$$\dot{\mathbf{X}} = f(\mathbf{X}, \mathbf{u}, \mathbf{W}) \quad (3.1)$$

The control inputs $\mathbf{u} = [\delta_r, \delta_s]^T$, consists of the rudder angle δ_r and the sail angle δ_s . The wind gets translated to sail forces $\mathbf{F} = [F_{forward}, F_{drift}]^T$, that consists of a forward force $F_{forward}$ and the drift force. This conversion is shown in Equation 3.2 but is further explained in Section 3.2. The true wind is as already mentioned explained in Section 1.5.

$$\mathbf{F} = g(\mathbf{X}, \mathbf{u}, \mathbf{W}) \quad (3.2)$$

The state input to the mathematical model is defined using 6 parameters. The first two parameters represent the position of the boat since the boat can only move in the 2 dimensional plane these consists of an x -position and a y -position. The third parameter is the orientation parameter θ . The following two parameters are the two translation velocities, these are described as the forward velocity $v_{forward}$ and the drift velocity v_{drift} . The last and final parameter is the angular velocity ω . This leaves a state representation according to Equation 3.3.

$$\mathbf{X} = (x, y, \theta, v, v_d, \omega)^T \quad (3.3)$$

Equations of Motion

The equations of motion captures the dynamic of the boat and the reference frame is described in Section 1.5. The catamaran and its constants are shown in Figure 3.1 to visualize the different constants that are put into the model. The model is brought forward using Newton's second law, $F = ma$.

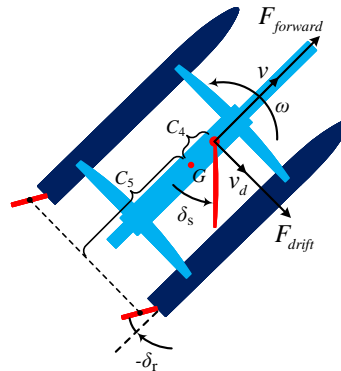


Figure 3.1 The catamaran model sailboat with the input parameters used for mathematical modeling

The translation in the x -direction is calculated using Equation 3.4(I), the y -direction is calculated using Equation 3.4(II) and the orientation of the catamaran θ is calculated using Equation 3.4(III). These three are fairly straight forward and are all depending on the remaining three equations. If one decomposes the translation one can see that this consists of the velocity going forward and the velocity going sideways. These velocities are defined in the boat coordinate system that is again already covered in Section 1.5. The velocities then intuitively have an influence of the translation based on the current orientation since the translation is defined in the world coordinate system.

$$\dot{\mathbf{X}} = \begin{cases} \dot{x} = & v \cos \theta - v_d \sin \theta & (I) \\ \dot{y} = & v \sin \theta + v_d \cos \theta & (II) \\ \dot{\theta} = & -\omega & (III) \\ \dot{v} = & \frac{F_{forward} - C_1 v - C_2 |dr| v}{M_{tot}} & (IV) \\ \dot{v}_d = & \frac{F_{drift} - C_3 v_d}{M_{tot}} & (V) \\ \dot{\omega} = & \frac{-C_6 C_5 v^2 \sin \delta_r \cos \delta_r - C_4 F_{drift} - C_7 \omega}{J_{tot}} & (VI) \end{cases} \quad (3.4)$$

The earlier mentioned v_{drift} and $v_{forward}$ are the same as the values v_d respectively v used in Equation 3.4.

Tangential Acceleration

Sail Forces When it comes to tangential acceleration one can define this using two sets of equations. Equation 3.4(IV) represents the directional acceleration. One can neglect all forces acting in the vertical direction since the assumption of no vertical movement has been made. The sail force acts on the canvas through the

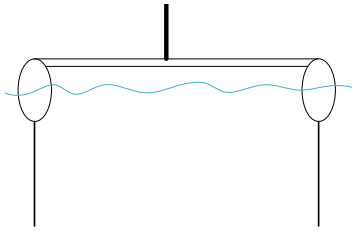


Figure 3.2 The catamaran model sailboat with focus on the dagger board foils mounted on the bottom of the hull to reduce drift

mast and the small force that comes from the sheet can be neglected based on the fact that applied forces from the mast is of much higher magnitude and do act as a proportional measure as the remaining constant parameters could take the absence of this force into account when tuned, similar to the assumptions made by [Jaulin and Bars, 2013], one can then merge the two sails and combine them to one sail force acting through the mast, this is illustrated in Figure 3.1. This sail force is decomposed to two forces earlier mentioned as $F_{forward}$ and F_{drift} both of these act and influence one of the velocities. How these forces are calculated and brought forward is explained in Section 3.2.

Frictional Forces When it comes to decelerating forces one can draw the conclusion that these mainly consist of hydrodynamic forces. These forces are of course also depending on the design of the boat. The deceleration force can be modeled as proportional to the velocity of the boat, like in [Fossen, 2002] and therefore depending on the directional velocity and the shape of the boat in that direction one can use a parameter for drift and one for forward movement. These parameters are defined as C_1 and C_3 , C_1 for forward movement and C_3 for drift. C_3 will render a larger value than C_1 since the shape of the boat favors a forward translation rather than a drifting motion due to the centerboards and rudders mounted beneath the boat shown in Figure 3.2.

Friction from Rudders The decelerating force not yet mentioned is the rudders used mainly for changing the heading angle. As one can imagine even these will decelerate the boat, the magnitude of this force does not only depend on the velocity of the boat but also the angle in which these will be actuated to have. A larger absolute angle with reference to which is shown in figure 3.1 will slow down the boat more. Therefore a simplified decelerating version is chosen and the C_2 parameter identifies the magnitude of this force. The rudder decelerating force can be described using Equation 3.5 and is presented completely in Equation 3.4(IV).

$$f_{\text{rudders}}(\delta_r) = C_2 F_{\text{rudders}} |\sin \delta_r| \quad (3.5)$$

It is common to not take these rudder forces into account when referring to translation but they are in fact a very important factor as one can see when observing how

they constantly minimize the rudder size to improve boat speed in competitions like the America's Cup¹. However, when it come to the drift motion this can be ignored. Since the rudder foils are already included in the drag parameter and the fact that the rudder angle is in the low $\delta_r \subset [-30, 30]$ degrees one can simplify this so just the constant C_3 parameter to reduce calculations and ignoring the δ_r -part.

Angular Acceleration

Given that the motion is limited to a 2-dimensional plane one equation describing the angular acceleration will be enough since the rotation is limited around one axis. It is in these tests assumed that the Center-of-Gravity (CoG) coincides with the Center-of-Rotation (CoR). The forces influencing the angular acceleration are the rudder forces, F_{drift} from the sails and a hydrodynamic force counteracting a rotational movement.

Sail Torque Starting with the force from the sails, only F_{drift} will affect any rotational movement since $F_{forward}$ acts through the CoR. The displacement of the F_{drift} force is included in C_4 parameter. The forces are transformed into torque about the CoR and in Section 3.1 the calculations of the moment of inertia and mass is explained. The torque τ_s , from the sails can be calculated using Equation 3.6. The total torque can then be presented in angular acceleration $\dot{\omega}$, together with the moment of inertia J .

$$\tau_s = F_{drift} C_4 \quad (3.6)$$

Angular Friction The rotational counteracting torque is proportional to the rotational velocity, ω . This decelerating force can be taken into consideration with the proportional parameter C_7 . This proportional method of modeling the counteracting torque is also used by [Fossen, 2002] and has been used successfully by [Jaulin and Bars, 2013].

Rudder Torque Now more about the main and most important source of rotational influences, the torque from the rudders. This is the main part that one uses to influence the boat heading. If the boat is well balanced with the sails and weighting, then one can expect all other rotational forces to be close to zero given that the rudder angle is zero. A constant goal with competitive sailing is to keep these forces so well balanced that the skipper of the boat can keep the rudder in the neutral position when wanting to go straight. The reason for this has already been presented in Section 3.1 when the decelerating force from the rudders was discussed. The torque from the rudder is calculated using the estimations that the rudders can be modeled as thin foils and that the torque will be zero at both $\delta_r = \pm 90$ and $\delta_r = 0$. With the displacement from the CoR to the Center-of-Effect (CoE) of the rudders assigned to the constant value C_5 and the magnitude of how much the rudder influences estimated to be constant and modeled into the constant value C_6 one can present the

¹ America's Cup is a sailing competition from 1851, were the competitors has the ability to design their boats under just a few regulations, making boat design one of the key elements to winning.

rudder torque using Equation 3.7. Given that the rudder can be modeled as a thin foil the force created will be squared to the boat speed v .

$$\tau_r = C_6 C_5 v^2 \sin \delta_r \cos \delta_r \quad (3.7)$$

Through combining these forces and torques one can determine the angular acceleration of the boat using the relationship of the torques, moment of inertia and angular acceleration presented in equation 3.8.

$$\tau = J \dot{\omega} \Leftrightarrow \dot{\omega} = \frac{\tau}{J} \quad (3.8)$$

Mass and Moment-of-Inertia

To determine the mass m , of the boat two versions were setup. one to calculate the mass of each hull m_{hull} , and summing these together to find the total mass and one just using the total mass directly. This is done so that an accurate moment of inertia can be calculated. The moment of inertia is calculated using the estimation that the hulls are rectangular blocks with a displacement from the CoR. With the use of Equation 3.9 for the moment of inertia at CoM for each hull and Equation 3.10 for the moment of inertia of a displaced mass to the total CoM, one can calculate the total moment of inertia using Equation 3.11.

$$J_{\text{hull}} = m_{\text{hull}} \frac{\text{Width}_{\text{hull}}^2 + \text{Length}_{\text{hull}}^2}{12} \quad (3.9)$$

$$J_{\text{displacement}} = m_{\text{hull}} \left((\text{Width}_{\text{boat}} - \text{Width}_{\text{hull}}) \frac{m - m_{\text{hull}}}{m} \right)^2 \quad (3.10)$$

$$J_{\text{tot}} = J_{\text{hull, right}} + J_{\text{hull, left}} + J_{\text{displacement, right}} + J_{\text{displacement, left}} \quad (3.11)$$

3.2 External Forces

What makes autonomous sailing such an interesting and difficult research topic is that it has unlike most other robotic research fields a propelling force that is not only impossible to control but also highly dynamic. This part covers how the wind propels the boat and how it can be translated to forces that are easy accessed by the mathematical model. Some earlier made research projects use the estimation that the sail can be modeled as a thin foil just like the rudder, these are presented in Section 2.3. Given the fact that the sail is made by some arbitrary fabric and that it constantly changes its shape based on the wind this foil estimation might not be as good as expected. Not so long ago sailors even used cotton sails that shrunk when exposed to water, luckily this is not the case any longer. The competitive America's Cup boats has even transferred to using rigid foils.

This project proposes a new method that measures the real forces created by the sails when exposed to wind. With the improved accessibility of sensors one

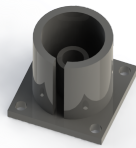


Figure 3.3 The mast and sails are attached in the hole of this 3D-printed part is printed using an Ultimaker 2+. One can attach the OPTO force sensor underneath this hole and use this to sense the wind.

could find a sensor that perfectly fit the requirements set by the project. Therefore one could measure the force instead of estimating it. One significant benefit of this method is that one no longer needs to measure the wind with a wind sensor. These are typically large and can be subject to many disturbances from the sails for instance. One can now use this method to retrieve forces and translate this to what wind the boat is exposed to. This is given that the developed model transforms the wind to forces and that it can be used in the reverse direction.

Force Sensing

Instead of using an estimation for how the wind translates to sail forces the approach of measuring the force directly is chosen. It is for this method estimated that the forces acting from the sheets and stays² can be neglected, it is also assumed that it can be modeled as one sail. One should also expect a momentum by the foot of the mast since the forces have their center of effect somewhere in the center of the sail for both sails. Given the fact that rolling motion is neglected one could discard this momentum and assuming that the sails are balanced to have the vertical momentum close to zero one could also neglect this.

To determine the forces at the relevant wind condition the OPTO force sensor is used. The force sensor is attached to the foot of the mast using a small 3D-printed part shown in Figure 3.3. Any rotational motion of the mast can be limited with the use of this small part since the boom carefully fits into the grove. This small part is one of the key components since it is used to model the sail and its forces.

When the mast, sail and sensor is mounted together the experimental extraction of the model of the sail can be started. From exposing the sail to varying wind conditions the specific sail forces can be extracted. After the experiments described in Chapter 6 the model that was used for the sail was developed. The sail forces F_x and F_y are generated from a given apparent wind angle and wind speed. The sail

² Stays are wires used to keep the mast upright, they often attach to the hull and the top of the mast. The forces are so small that thin threads are used on this catamaran.

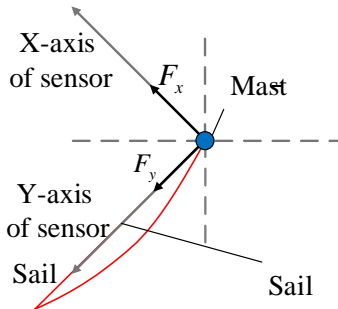


Figure 3.4 F_x and F_y forces in the sail frame display.

forces are shown in Figure 3.4 and are in reference to the sail. The setup that was used is shown in Figure 6.1.

After the sail forces have been extracted one needs to translate these into drift and forward forces in the boat frame since the boat frame is used in the model calculations when determining the dynamic properties. For the forward force one can use Equation 3.12, this is periodical given the angle usage. The drift force is calculated using Equation 3.13 and is similar to the previous equation.

$$F_{forward} = -F_y \cos \delta_s - F_x \sin \delta_s \quad (3.12)$$

$$F_{drift} = F_y \sin \delta_s - F_x \cos \delta_s \quad (3.13)$$

Real Sail Angle, δ_s

One important step before calculating the sail forces is to determine the actual sail angle. Another factor that complicates the modeling of the boat is the fact that the sail angle can not always be controlled either. Given the fact that the sheet for controlling the sail is unable to withstand any pushing forces one can not completely control it. If the wind was to attack the sail from the outside creating a pushing force on the sheet a new sail angle will be created and this must be taken into account before calculating the sail forces. Depending on the configuration of the sail and the apparent wind one can determine a new real sail angle this is calculated using Equation 3.14 where the apparent wind angle is rotated 180° to match the reference angle of δ_s .

$$\delta_s = \begin{cases} \psi_{w,apparent} & if |\psi_{w,apparent}| \leq |\delta_s| \\ -\delta_s & elseif \psi_{w,apparent} \leq 0 \wedge \delta_s \geq 0 \\ -\delta_s & elseif \psi_{w,apparent} \geq 0 \wedge \delta_s \leq 0 \\ \delta_s & else \end{cases} \quad (3.14)$$

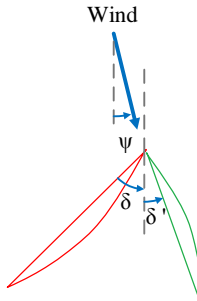


Figure 3.5 An example scenario of how the controlled sail angle can differ from the real sail angle. The red sail is the controlled sail and the green is the real. The dotted line is the directional center line of the boat with the upward direction towards the bow.

To display what occurs when an invalid sail angle is set Figure 3.5 was brought forward. The control input is set to a positive value while the wind attacks the sail from the outside which will create a new sail angle based on the current situation. The sail angle will in this case be set to the same direction as the apparent wind due to the invalid setup. The red sail position is the invalid and controlled one and the green is the one that is the real sail angle. The new sail angle is set to $\delta' = \psi$.

Force Polar Diagram

When it comes to modeling and especially path planning for sailboats in general, it is common to use a so called velocity polar diagram to determine what direction to sail to. Research projects for autonomous sailing use this to optimize the boat path, one group that uses this is the team behind AEOLUS from Eidgenössische Technische Hochschule (ETH) Zürich [M. Tranzatto, 2015b]. This velocity polar diagram determines the velocity made good for the specific sailboat at different wind speeds. An example of a downwind velocity polar diagram from [Textor, 1995] is shown in Figure 3.6. The red dots show the optimal downwind velocity for an arbitrary sailboat at different wind speeds. What one can observe is that the fastest heading for going downwind changes depending on the wind speed and that given the design of the boat, going straight down wind might not be optimal even though the target position is located straight down wind.

What is proposed here on the other hand is to use the forces directly to determine the control inputs. With the collected force data one can create a Force Polar Diagram (FPD). These are extracted through the experiments explained in Chapter 6 and a set of test data is shown in Figure 6.3 and 6.4. These are shown in the sail coordinate frame and can be used to extract a velocity polar diagram through iterating through the different angles of attack for the wind. One could also simply decompose the FPD for both axes and combine these to create the forward and drift

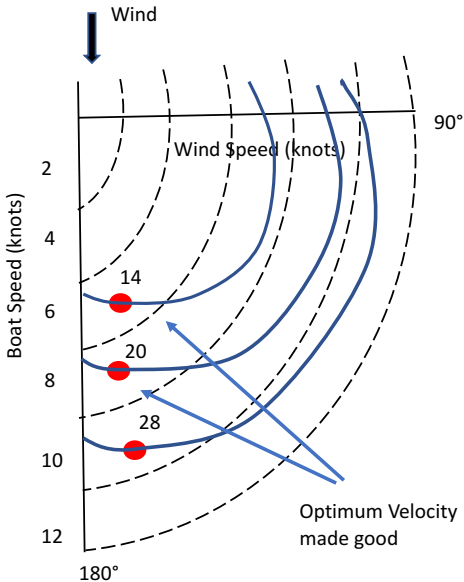


Figure 3.6 A Velocity Polar Diagram for an arbitrary sailboat. The curves display the velocity made good of a boat at different wind conditions. This is commonly used for determining what heading one should set to reach a position as fast as possible. The fastest downwind heading is shown by the red dots.

forces used in the model ($F_{\text{forward}}, F_{\text{drift}}$). The sail angle that then creates the largest F_{forward} could be set as the control input. This approach is new to the concept of autonomous sailing but fails to determine an optimal heading angle and is therefore flawed unless a sail angle is chosen and then a heading is determined to optimize the velocity made good based on it.

3.3 Parameter Identification

The Model Parameters [$C_1 \dots C_7$] are to be determined to make sure that the mathematical model corresponds to the real world boat. When the model has been setup there still needs to be some adjustments to make it fit the real boat, some of these can be measured directly on the boat and some parameters need to be determined through experiments. In this part each parameter is explained and experimentally or algebraically calculated.

Table 3.1 Non Experimental Parameters. Parameters not determined through tests or simulations.

Parameter	Abbreviation	Value	Entity
Boat Mass	M_{tot}	0.6	kg
Moment of Inertia	J_{tot}	0.0130	m^2kg
Mast Displacement	C_4	0.03	m
Rudder Displacement	C_5	0.20	m

Non Experimental Parameters

A few of the parameters can be determined before even launching the boat into the water. The mass and moment of inertia calculations are explained in Section 3.1. The mass was evenly distributed over the two hulls during the tests which made the algorithm calculating the moment of inertia use the simplified calculation method.

The other set of constants that were determined using measurements are the different distances. The rudder's force has a displacement with regard to the axis of the boats CoR, this was measured and assumed to be at a constant distance from the CoR. The distance to the mast was also assumed to be constant even though different sail angles will change the center of mass for the rig. These two parameters C_4 and C_5 are shown in Figure 3.1.

All these non experimental parameters are shown in Table 3.1 and was measured prior to any experiments.

Experimental Parameters

The remaining five parameters and how they are selected is presented in this Chapter 6. $[C_1, C_2, C_3, C_6, C_7]$ are all coefficients of some kind and are to be chosen to optimize the mathematical model. An initial guess of the parameters was made and with the experience of a sailor and the design of the boat some relations between them can be set. The boat will be less prone to movements perpendicular to the direction and a catamaran is less maneuverable around its axis of rotation than mono-hulled boats.

The parameters are more precisely set in Chapter 6, other than determining these relations and performing a qualified guess of what the parameters might be. Through a number of experiments and tests the mathematical model is to be carefully fitted.

4

Control

An approach to controlling the sails and rudders is presented in this chapter. With a predefined desired heading the approach to determining the controlled rudder and sail angle to maximize the speed in that direction is brought up here. One can use methods with varying levels of complexity, one approach is to use a controller that is based on fuzzy-logic, another method would be to use a nonlinear controller approach and in addition to this previous research has proven that even linear approaches can be successful in similar applications [M. Tranzatto, 2015a].

A control method is proposed here with reference to the expression of a PID controller. For this particular scenario it is initially started using the general Equation 4.1 for PID control.

$$u(t) = K_p e(t) + K_i \int_0^t e(t) dt + K_d \frac{d}{dt} e(t) \quad (4.1)$$

The control output $u(t)$ is calculated with reference to the proportional part which impacts the control based on the K_p constant. The integral and derivative parts influence the control by their constants K_i respectively K_d . The error, $e(t)$ is determined based on the desired heading, current heading or current Course over Ground (COG). The error and how it is calculated is rather complex and will be explained further in Section 4.1. As objectives of sailing voyages might be for long distances the simple difference between the desired and current heading might not be enough.

The general expression for the PID controller can be rewritten to match the calculations in discrete time. Then the control work the same way as in Equation 4.1 through using the new Equation 4.2.

$$u(k) = K_p e(k) + K_i \sum_0^k e(k) \Delta t + K_d \frac{\Delta e(k)}{\Delta t} \quad (4.2)$$

Where k denotes the step instead of t as in time. $\Delta e(k)$ is the difference between the errors for each step.

4.1 Heading Error

The general way of calculating the control error is through using Equation 4.3. $r(t)$ is in this situation the reference, which means the desired heading and $y(t)$ is the current heading of the boat.

$$e(t) = r(t) - y(t) \quad (4.3)$$

This section is regarding the error used in the control calculations. When it comes to heading error the most intuitive and a common way to calculate it is to just take the orientation of the boat and put this in relation to the desired heading. To mention one piece of literature that uses this is the people behind [Jaulin, 2012].

This direct approach is rather simple and the heading error is calculated using Equation 4.4.

$$e = \theta_{\text{des}} - \theta \quad (4.4)$$

However, these calculations might not be as accurate as suggested. What the normal heading angle does not take into account is the drift. Since the boat is strongly limited by the wind one can not control it so that it goes towards the wind more than a certain angle. Because of this it might be desired that the boat heads more upwind than necessary, if the wind were to shift direction the boat might be forced to tack to reach the desired target. If the heading were higher in the first place this could have been avoided. This is illustrated in Figure 4.1, it shows how an unnecessary decelerating and time consuming set of tacks could be avoided with another control strategy.

Instead of using the heading angle one could use the actual COG of the boat, given that the desired heading is the direction of travel that is the heading one wants to achieve. Since the absolute drift velocity of the boat typically is separated from zero the translation of the boat will not be in the same direction as the orientation of the boat and the direction of travel that it has. Given that it is separated from zero one can use similar calculations as used when calculating the apparent wind and base the heading error on this.

An illustration of how the COG can differ from the boat heading based on the impact of a drift motion is shown in Figure 4.2.

The straight forward error is calculated using Equation 4.4. To calculate the error when the drift is considered one can use Equation 4.5.

$$e = \theta_{\text{des}} - \left(\arctan \left(\frac{v_{\text{drift}}}{v} \right) + \theta \right) \quad (4.5)$$

Equation 4.5 works the same way as using Equation 4.6 which captures the movement of the boat directly instead of using the drift and forward velocities.

$$e = \theta_{\text{des}} - \arctan \left(\frac{\dot{y}}{\dot{x}} \right) \quad (4.6)$$

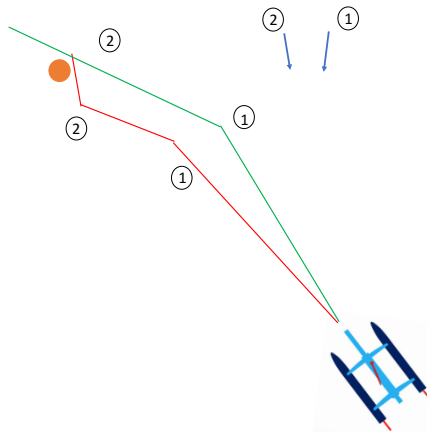


Figure 4.1 Example scenario of how a wind shift can impact an incorrect heading angle. State 1: Wind from right, red trajectory heading straight towards the target position and green trajectory heading slightly higher towards the wind. State 2: Wind shift to left, red trajectory needs to perform two tacks to complete the mission of reaching the mark and green trajectory reaches the target without making any major maneuvers.

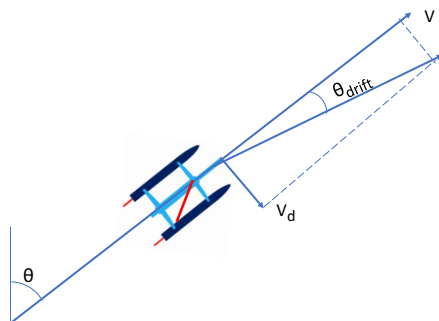


Figure 4.2 How the Course over Ground is affected by the drift velocity. The real heading is the sum of θ and θ_{drift} .

Since the bearings and headings are set in cylindrical coordinates it is necessary to make sure that the right heading angle error is communicated. With the help of Algorithm 1.

Result: Returns correct heading angle error, negative values if a left turn is necessary and right turn if values are positive.

```

while  $t < t_{simulation}$  do
    if  $\theta_{des} < 0$  then
        |  $\theta_{des} = \theta_{des} + 360;$ 
    end
    if  $\theta < 0$  then
        |  $\theta = \theta + 360;$ 
    end
     $\theta_{des} = \theta_{des} - 180;$ 
     $\theta = \theta - 180;$ 
     $Error = \theta_{des} - \theta;$ 
    if  $Error > 180$  then
        |  $Error = Error - 360;$ 
    end
    if  $Error < -180$  then
        |  $Error = Error + 360;$ 
    end
end
```

Algorithm 1: Pseudo code of determination the correct heading error with regards to both cylindrical coordinates and smallest angle.

This calculates the heading error, $Error$ based on the desired heading angle, θ_{des} and the current heading, θ whether this is calculated being the COG or the straight forward orientation depends on computational capacity.

4.2 Control Outputs

This section covers how the actual control outputs are set, they both have saturation's and the sail is also limited by the wind as mentioned in Section 3.2. When carefully observing the mathematical model one can notice that the sail actually influences the angular acceleration and could therefore be used to change the heading of the boat. When it comes to conventional sailing it is more than common to use this when changing the boats heading in a more significant magnitude. This can be observed even more clearly when it comes to sailing on ice, even though the runners on the ice-yacht is limiting the rotation of the yacht one always need to carefully adjust the sail angle when changing direction from sailing upwind to downwind. If one

Table 4.1 Non Experimental Parameters. Parameters not determined through tests or simulations.

Controller	K_P	K_I	K_D
P	1.1	-	-
PD	1.76	-	0.25
PID	1.32	1.0	0.25

fails to do so and the wind speed is high enough this can lead to the yacht tipping over because of the strong forces, which can be observed in certain sailboats.

Rudder Angle

With the calculated heading error from Algorithm 1 the error is within $Error = \pm 180^\circ$. The rudder angle is limited to $\delta_r \pm 30^\circ$ from the actuator. One can set up a proportional controller with the error, given the coordinate system of the rudder and the setup of the actuator a positive δ_r will generate an increased heading angle in the world frame.

For this application three sets of controllers were brought forward. all hold the output condition to satisfy the actuator limit meaning, $\underline{u} \leq u(t) \leq \bar{u}$. In addition to this one of the controllers used is a P controller, one PD and the other is a PID controller. All controllers were tuned heuristically and the forces from the sails were neglected for turning and therefore not included in the part controlling the heading. In the same way one can neglect the forces from the rudders when tuning the appropriate sail angle.

First the control output is contained by Equation 4.7, then the heuristic tuning of the parameters was done to achieve a stable and fast response.

$$u(t) = \begin{cases} \bar{u} & \text{if } u_{\text{des}}(t) \geq \bar{u} \\ u_{\text{des}}(t) & \text{if } \underline{u} < u_{\text{des}}(t) < \bar{u} \\ \underline{u} & \text{if } u_{\text{des}}(t) \leq \underline{u} \end{cases} \quad (4.7)$$

The gain parameters were tested through a number of tests brought forward in Chapter 6. Diffrent combinations were found to be successful in the different scenarios, all combinations of these are shown in Table 4.1.

The approach used for tuning the parameters is from the classic Ziegler-Nichols rule and generated a good result for this application. The values for the ultimate gain K_u is 2.2 and the oscillation period T_u was set to 2s.

Sail Angle

When it comes to setting the appropriate sail angle a number of different approaches have been taken, one of the most common way of doing so is to just set the sail angle proportional to the apparent wind angle. This method was used by [I. Giger, 2009]. What is proposed in this section on the other hand is to set the sail angle based on

the FPD and how it can maximize the surge. The appropriate sail angle can be set from the FPD, the tuned mathematical model testing through the different angles to find the most optimal sail angle for the boat.

The sail angle is controlled by an actuator inside the hull of the boat. This actuator can only control the sheet which is either stretched or loose. The sail angle can be controlled directly in the simulation environment but in the real configuration it must be considered that the sheet is straight and not bent like an arch. To translate the control from the actuator to a real sail angle some small calculations must be done. With the use of the cosine rule, Equation 4.8 one can adopt this for this situation through Equation 4.9 and Equation 4.10. $d_{\text{mainsheet}}$ is the distance from the mast to the mainsheet boom bail and l_{sheet} is the length of the sheet. It is here assumed that the vertical displacement between the boom of the main sail and the deck where the mainsheet leaves the boat is so small that it can be neglected.

$$a^2 = b^2 + c^2 - 2bc \cos A \quad (4.8)$$

As far as it comes to the control of the sail angle, this will be predefined and controlled by both apparent wind angle and apparent wind speed given the relevant FPD, which is calculated using Equation 4.9.

$$l_{\text{sheet}} = \sqrt{2d_{\text{mainsheet}}^2(1 - \cos \delta_s)} \quad (4.9)$$

$$\delta_s = \arccos \left(\frac{l_{\text{sheet}}^2}{2d_{\text{mainsheet}}^2} + 1 \right) \quad (4.10)$$

With consideration to the fact that the mathematical model has a set of assumptions underlying one can draw the conclusion that even though the set sail angle is mathematically the best sail angle it might not be the best sail angle in reality. It is therefore proposed that the set angle is used only as an angle of reference and used to set an initial sail angle. When the boat is on a steady course and steady state one can alter the fixed sail angle to find a new optimal one given the current conditions. With the basis of a sailors experience it is known that the sail angle should be larger if the sea is rough. Factors like these are not considered in the model or in the FPD but are covered more thoroughly in Chapter 6.

5

Optimal Trajectory Control

So far all but the guidance of the catamaran has been mentioned, in this section it is determined what reference angle the controller receives and the basis of the decision making behind it. What is already explained multiple times in Chapter 1, 3 and 4 is here explained further and determined how to get around, the constraint of the wind, avoiding obstacles and optimizing the trajectory from one point to another.

This section presents an approach to minimizing the time and maximizing the level of safety when on the voyage from one location to a predefined target location. This method was developed with the use of previous works and their shortcomings, especially given the success from [M. Tranzatto, 2015a; Pêtrès et al., 2015]. However even these have shortcomings and discard some important decision making information.

5.1 Path Planning Algorithms

A description of the existing methods to planning the boats path is done in this section of the chapter. This path planning for navigation on water leaves some common approaches unusable and even more methods highly unsuited when limited by the wind. With the existing research projects already performed only a few of the existing path planning algorithms have been used. One can often find some short coming with the existing method that makes it difficult to apply to autonomous sailing.

The main reason why many algorithms are unfit for this application is as mentioned, the wind. Leaving everything to the power of the wind constraints all operations.

Potential Field Method

One approach to solving this problem is using the so called Potential Field Method. This method has been used successfully on autonomous sailboats in the past, one in particular is presented in [Pêtrès et al., 2015]. This method uses forces to determine the desired heading of the boat, any obstacle or undesired location is assigned a repelling force. The target location or locations that are favorable to sail through

are assigned attractive forces. With the help of assigning these forces the charge around the boat with the smallest total cost can be selected as the desired heading or location. Through introducing a fixed repelling force from the no-sail zone sailing straight towards the wind can also be avoided.

The researchers in [Pêtrès et al., 2015] also solve the issue of stranding in a local minimum through assigning a repelling force at the boat location which leads to the boat always wanting to change location. When the repelling and attracting force act so that they cancel each other out it can lead to the boat staying at one location.

One of the great benefits of using this strategy is that obstacles or any repelling force that are distant from the boat have little or no effect on the path planning. With the wind being as dynamic as it is it can lead to an obstacle not being an obstacle in the future. If the boat were to go straight towards an obstacle that are very distant from the boat it might lead to the wind changing direction and leaving the obstacle far away from the previous path since the boat potentially could go higher and avoid the obstacle without any unnecessary maneuvers.

Another great benefit from using this method is that one can also assign forces that are similar to the wind. As mentioned in Chapter 3, a higher wind speed will result in higher sail forces propelling the boat. Therefore, it is also desired to sail where the wind speed is as high as possible with the exception of sailing in to storms and hurricanes which might cause damage. To take this into account when determining the path one could simply assign an attracting force to an area with higher wind speeds. In Figure 5.1 the wind speed is plotted for the pool where the experiments were conducted. The wind is strongly concentrated to the fans at the end of the pool and gradually decreases as one reaches the opposing end. It might therefore be desirable to sail closer to the fans if one is crossing from one side to the other.

Polar Diagram Method

A sailboat is unable to sail straight upwind, and with the use of the velocity polar diagram presented in Section 3.2 and shown in Figure 3.6 this can be considered. Because of this limitation all upwind sailing must be performed with an angle to the apparent wind. This will create a trajectory that makes the boat go zigzag. When observing the velocity polar diagram figure one can see that the maximum boat speed achievable is strongly depending on the heading of the boat in relation to the apparent wind. This means that the speed that the boat can be set as a function of its apparent wind angle. However, this is if the waves, currents and more are disregarded.

This diagram of velocities at different heading angles is the base of the path planning. It takes all possible headings and calculates all the relative velocities toward the target. The heading which gives the highest velocity made good (VMG) is the one chosen for arriving at the target position as fast as possible. Since the heading straight towards the wind is theoretically zero and even negative in practice this heading will not be chosen.

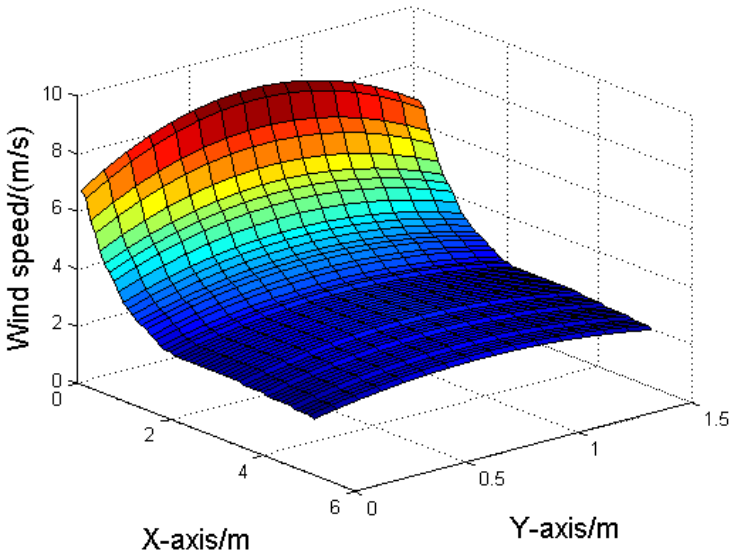


Figure 5.1 Plot of the wind field in the pool used for experiments. To aid use of the potential field method favoring places with higher wind speeds.

There are only a few reasons why one might not use this approach. It does however neglect some dynamics of the boat that really should be taken into account. As brought up in Chapter 3, increasing the rudder angle will introduce a decelerating force. This means that any change in direction will slow the boat down, this method does not consider this. Neither is the cost of making a maneuver like a tack or a gybe. During these actions one does not only slow the boat down because of the increased rudder angle but also because of the inefficient sail angle forced upon the boat configuration.

This method was modified to avoid obstacles by assigning the boat speed towards any obstacle to zero. This ensures that the boat will not choose that direction of travel and the obstacle is avoided. This method was implemented by [Stelzer et al., 2011] and was proven to be working on their Roboat shown in Figure 5.2 from [[roboat_img](#)].

Other Methods

Some other methods that have been used in the past are briefly mentioned in this section. ENESTA Bretagne presents a control method that is based on a petri net approach when it comes to the decision making. Their work is presented in [Clement, 2013].

The team behind Robbe Atlantis implemented a fuzzy logic control system with



Figure 5.2 ASV Roboat, developed by Austrian Society for Innovative Computer Sciences which uses the Velocity Polar Diagram for planning it's path

two Mamdani type fuzzy interface systems that was also proven to be successful [Stelzer et al., 2007].

A very basic method using a simple two level state machine was used by the team behind [Briere, 2008], the lower level controls the rudder and sail angle and the higher level is used for maneuver control.

5.2 Multi-Variable Path Planning

From the research behind AEOLUS, the autonomous sailboat developed by ETH Zürich an approach using a different costs was presented [M. Tranzatto, 2015a]. With the fundamentals from what IFA did with AEOLUS this method was developed. In this section the cost based trajectory control algorithm is highlighted and explained. The basis of this model is from the Polar Diagram Method and has been enhanced to improve the performance.

Costs

In the cost function method this method takes multiple costs for different paths into account when making the decision on what path to take. Normally the major decisions are made by the helmsman, tactician or strategist. These three often have different responsibilities that overlap and together the goal of their work is to complete the predefined array of target way points. The helmsman ensures that the boat is sailing at an optimal speed given the desired heading. The tactician and strategist have more similar tasks and together they set the desired heading. The difference between the two is that the tactician has a shorter range and decides on decisions like what side to avoid an obstacle. Meanwhile the strategist decides on longer decisions like what side of the course to sail on or what direction to sail towards. With this desire from the strategist the tacticians goal is to make sure that the boat goes there fast and without any complication and the helmsman focus on boat speed.

These tasks can be integrated if the crew is small or even necessary when the crew is limited to one person. The basis of the decisions made by the tactician and

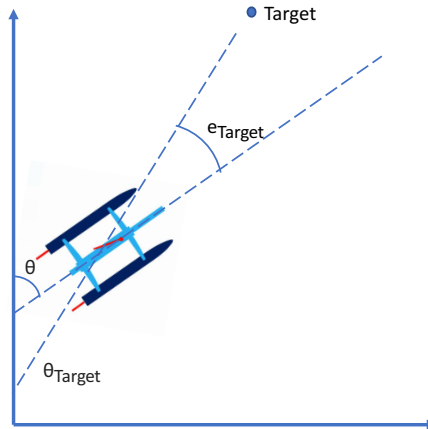


Figure 5.3 Figure showing the different angles and heading errors. for the catamaran sailing towards a target.

the strategist are the so called costs, the minimum accumulated cost for all headings is the heading the helmsman receives and his work is described in Chapter 4. All these accumulated costs are normalized to make the tuning process easier.

Heading Cost

First all costs are explained and later it is described how the combination of them all is to be performed. In this section the most important cost is explained, the Heading Cost. This is the most important one since it is the only one that makes the boat go towards the target position. It is also the only negative cost when approaching the target as it unlike all other actually improves the state of the boat, and it is minimized when sailing straight towards the target and maximized when sailing in the opposite direction.

This cost is the most straight forward as it is in the interval $[-1, 1]$, -1 is going straight towards the target and 1 is sailing in the opposite direction. It can be calculated using Equation 5.1 to calculate the heading error between the current heading and the bearing towards the target. θ_{Target} as the bearing to the target in the world coordinate frame. These different angles are shown in Figure 5.3.

$$e_{\text{Target}} = \theta_{\text{Target}} - \theta \quad (5.1)$$

With Equation 5.1 and Equation 5.2 the value of the target cost can be calculated.

$$TC = -\cos e_{\text{Target}} \quad (5.2)$$

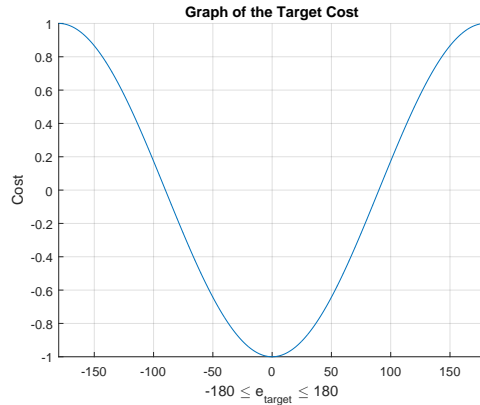


Figure 5.4 Graph of the Target Cost, x-axis is the e_{Target} and y-axis is the cost

This means that if the heading angle does not deviate from the bearing of the target the target part is minimized and negative. When the boat is heading away from the target a larger cost is introduced and it will lead to a positive cost. This cost can be visualized with Figure 5.4 and has the cost on the y-axis and the heading error on the x-axis.

Velocity Polar Diagram Cost

In this section the second most important cost is explained, the Velocity Polar Diagram Cost. The Velocity Polar Diagram is described in Section 3.2. To better understand this cost one might refer to the Polar Diagram Method in Section 5.1. This cost is minimized when the speed of the boat is maximized. The speed of the boat can be calculated using the current wind conditions and through these one can make use of the predefined speeds at different headings to determine what speed each potential heading might bring.

As the Polar Diagram Method advocate, using the wind angle as initial reference might be a good starting point for the decision making on the catamaran. What this cost does is that it is optimized when the sailboat theoretically would sail the fastest and it becomes sub-optimal when the boat sails slower.

Once the polar diagram has been extracted also this can be shown as a graph of the cost in relation to the heading angle like Figure 5.4. This polar diagram cost is shown in the graph in Figure 5.5.

Obstacle Cost

This section covers obstacle avoidance. [Stelzer et al., 2011] implemented a solution for this when using the polar diagram method. A rather simple way of dealing with

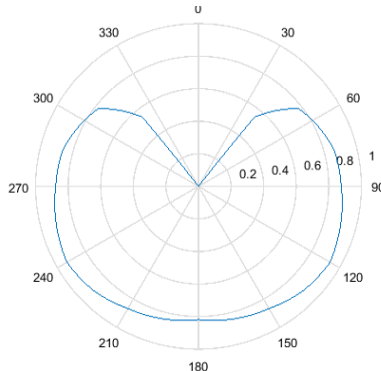


Figure 5.5 Graph of the VPD Cost, the boat speed is in relation to the wind angle

obstacles when using the polar diagram method was to alter the polar diagram and assign the VMG towards the obstacle to zero. The heading that led the boat towards the obstacle would then never be selected since most other headings had a better VMG, and therefore the obstacle would be avoided. What is proposed in this section is in some way similar to that solution.

A cost is created based on the location of the obstacle, if the obstacle is far away the cost will be lower. An example displaying a potential obstacle configuration is shown in Figure 5.6.

A visualization of this can be seen in Figure 5.7.

Unless obstacles are predefined or listed as land in maps, detection of them is still impossible. The catamaran is in need of hardware that can detect obstacles, this could be done through different methods, using an omni-directional camera or LIDAR.

Action Cost

Considering the dynamics of the boat and the wind forces from the modeling, one can recall that a rudder angle will introduce a decelerating force and the sails do not generate a lift force if the apparent wind angle is close to zero. This is exactly what occurs when a major heading change or an action (tack or gibe) is performed. A constant heading is therefore preferable.

This negative effect of changing course is implemented through an action cost. Assigning no cost to keeping a constant heading and a higher cost for a larger heading change will take care of this. The action cost is shown in Figure 5.8 and shows no cost to keeping the current heading and a high cost to turning $\pm 180^\circ$.

Strategic Cost

Race strategies are an important part of sailing as it is one of the critical parts of determining who will win races. As soon as sailing reaches a high level on compet-

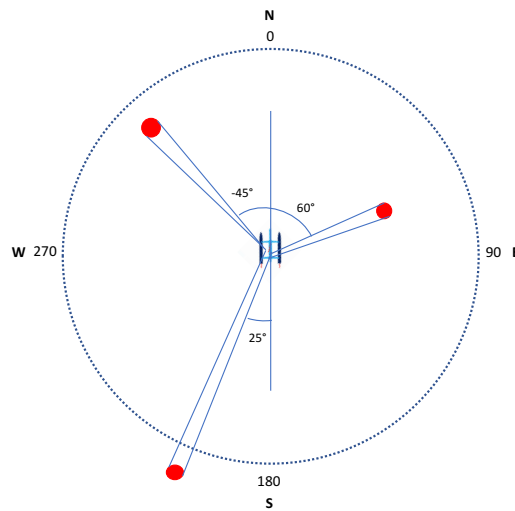


Figure 5.6 Graph of the Obstacles, the boat is located at the origin and the bearings of the obstacles are shown in the figure. These obstacles are related to the costs shown in Figure 5.7.

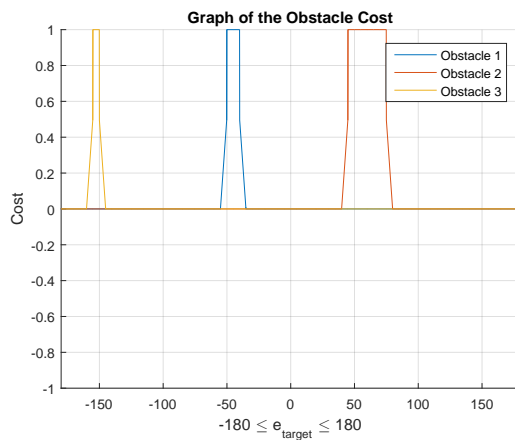


Figure 5.7 Graph of the Obstacle Cost, x-axis is the bearing towards the obstacle and y-axis is the cost based on a fictional configuration of obstacles shown in Figure 5.4

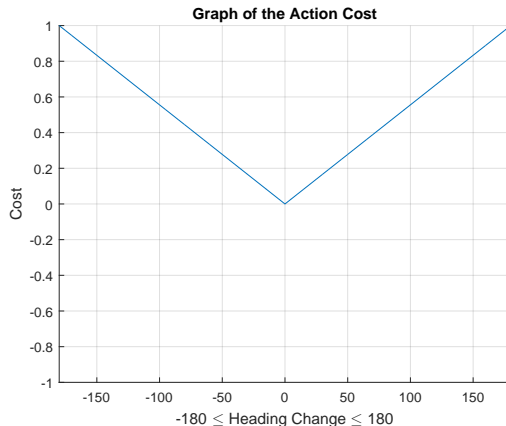


Figure 5.8 Graph of the Action Cost, x-axis is the heading change and y-axis is the cost.

itiveness, then boat speed is more or less similar which leaves tactics and strategies as the most crucial aspect.

This part describes an initial measure to make sure that the strategies are reasonable, strategies are infinitely complex as a strategist needs to consider wind fields, currents, course placement, landmass and more. This cost considers two important aspects, sailings right-of-way and the top-mark layline¹.

Right-of-Way According to the rules of competitive sailing, a boat coming from starboard has the right-of-way if approaching a boat coming from port. This would at first sight mean that one would prefer sailing on starboard tack. However, this is not the case when it comes to strategies. In a more long term perspective, just as mentioned above, one wants to approach other boats from starboard. This means that one must sail on port tack to be able to approach other boats, sailing on port tack will lead to the boat being positioned on the right hand part of the course and therefore approach boats from starboard when reaching the top mark. This cost is rather simple to implement and is shown in Figure 5.9.

Layline By the fact that the wind is dynamic and constantly change its direction, positioning oneself on the layline too early can be unfavorable. The explanation of this is that one always want to sail the shortest way to the target, if the layline changes its position due to a change in wind direction one might have been able to sail a shorter path. This is illustrated in Figure 5.10.

¹ Layline is the line which goes from the top mark and along the point in which one would be able to reach the top mark without having to tack

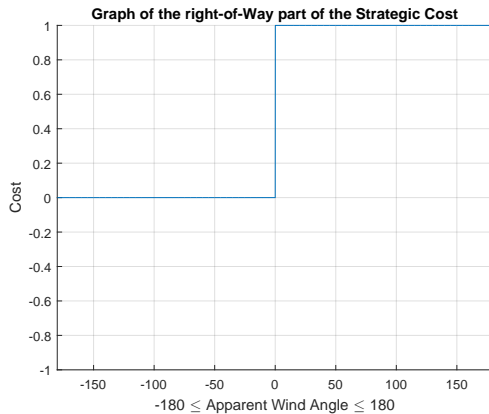


Figure 5.9 Graph of the right-of-way part of the Strategic Cost, x-axis is the Apparent Wind and y-axis is the cost.

This can be avoided using a cost that always favors the direction that leads towards the center of the course and gradually increases the further away from the center one is located.

Tactical Cost

This section discusses unlike the strategic part not where to position oneself but how to get there. As the wind can change direction with a rather constant frequency sometimes and maintain a constant mean wind direction over time, this could be used as an advantage.

What is proposed is to implement a stochastic optimal control that uses the assumption that one can model the wind direction as a Markov chain with decreasing probabilities of reaching a state with a higher deviation from the mean wind direction. As the polar diagram method already covers the apparent wind and therefore makes sure that the boat always sails with the highest VMG, then the current wind shift is also considered. What is desired is to detect future shifts just like the right-of-way part of the strategic cost tries to make sure that the boat sails on starboard tack in the future.

To determine this cost one has to iteratively find an optimal solution for the trajectory of the boat. Starting at the top mark, one can go backwards from N to step 1, the boat. Each time step one calculates the probable positions based on the Markov chain and the possible wind transitions. It is then based on the optimal and most probable path, what the cost should be to favor a heading in that direction.

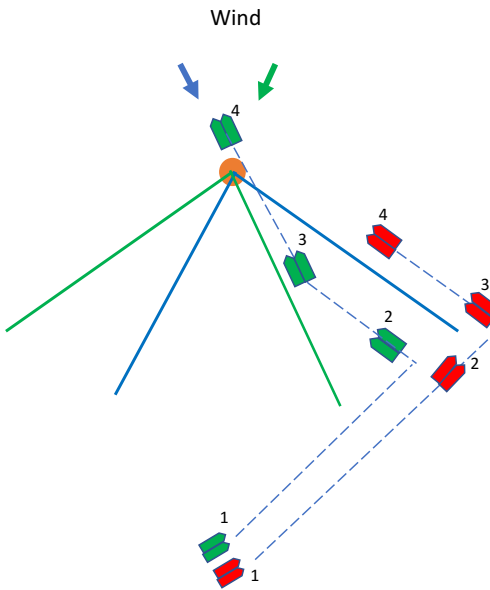


Figure 5.10 This figure show two different paths for the boat advancing towards the top mark. the wind is initially coming more from the left and then after position two it turns. The green boat tacks before the layline and still reach the mark, sailing a shorter path. The second boat does not favor sailing closer to the center and tacks later.

Additional Costs

Three costs yet to be deeper analyzed are in this section brought up. Waves direction and shape have a great influence on the boat speed, tactical positioning with regard to the other competitors is always of great value and long term wind conditions is always in the back of a competitive sailors head. There are of course infinitely many costs that could be implemented but as the number of costs increases so does the tuning complexity and the costs decrease in how much influence they actually have.

Wave Cost Waves are often neglected or already considered in the VMG determination in previous research projects. A common assumption is also that the waves move in the same direction as the wind, this is rarely the case though.

Sailing straight into the waves will slow the boat down drastically and sailing with the waves can also increase boat speed. What one therefore should do is to introduce a cost that looks like the wave cost in Figure 5.11. This cost has a maximum in the heading straight towards the waves and minimum going away from it. The amplitude of the cost is strongly correlated with the shape of the waves.

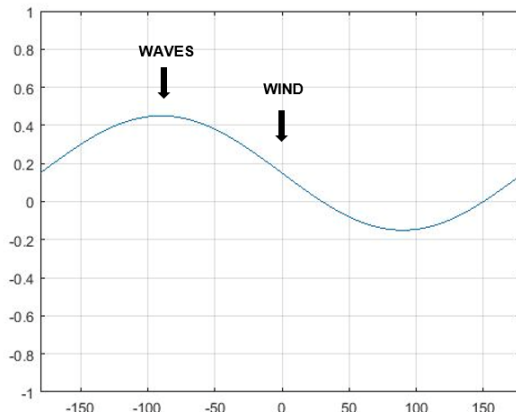


Figure 5.11 Graph of the Wave Cost, x-axis is the Apparent Wind and y-axis is the cost.

Tactical Positioning Cost This cost is implemented to minimize risk when in the lead and maximizing the risk when not in the lead since the risk and reward ratio is higher. The function of it is similar to the Layline cost, instead of using the center of the course as a center line one should use the mean location of the other competitors. This could be easily implemented through K-means clustering and will make sure that the boat stays between the competitors and the target to minimize risk. If one is located behind the competitors, then the principal is to change the cost so that it is not desired to stay close to the center line, simply the opposite to what was proposed earlier.

Long Term Wind Cost The longer the race or mission the more important are the actual weather forecasts. This cost is a rather strategic cost as it is similar to the other costs trying to position the boat on the course. One can manually introduce costs that favor the weather forecasts, if the wind is expected to change direction to the right, positioning oneself on the right hand side of an upwind leg².

5.3 Combining the Costs

All these costs need to be weighted and combined to reach the final decision on what desired heading to send to the controller. As each cost assigns a value to every specific heading, cost values that are in the interval $[-1, 1]$ independent of any tuning, a simple accumulated cost will not do.

² Leg is the different directions that one has to sail when going from one target to another, the two most typical ones are upwind and downwind legs.

To achieve the desired characteristics, each cost needs to be carefully weighted with a specific weight constant. The value of all weighting constants is in the interval $[0, 1]$.

As one can observe in Equation 5.3, the P_{HC} , VPDC has combined both heading and velocity polar diagram cost in one. This is because of the fact that the VMG is relative to the heading error and therefore one simply multiplies the two of them as a high velocity in the wrong direction should be negative. Considering this, one can calculate the total cost with Equation 5.3

$$C_{\text{tot}} = P_{HC, \text{VPDC}} C_{HC} C_{\text{VPDC}} + P_{OC} C_{OC} + P_{AC} C_{AC} + P_{SC} C_{SC} + P_{TC} C_{TC} \quad (5.3)$$

To calculate the desired heading from this one might use Equation 5.4. The heading angles that one might calculate the cost at can be reduced to decrease computations needed.

$$\theta_{\text{des}} \Leftarrow \begin{cases} \min(C_{\text{tot}}(\theta_C)) & \theta - 95^\circ \leq \theta_C \leq \theta + 95^\circ \end{cases} \quad (5.4)$$

5.4 Optimal Trajectory Control Analysis

To conclude this chapter, An example situation with the corresponding costs is presented. The boat is located like shown in Figure 5.12. The costs that are assigned in this situation is shown in Figure 5.13, 5.14 5.15 and combined with their weighting one can see the total cost in Figure 5.16. With this one can determine that the optimal heading angle is the same as the current heading angle and one should therefore keep sailing in the same direction. Same calculation can be made at the next location until the boat finally arrives to the target location.

5.5 Strategic Path Determination

What has been explained so far is the determination of a desired heading θ_{des} with a given target. In case when the target is far away, then the control algorithm might be more successful if this journey were to be split into multiple way point targets. There are situations when strong currents are to be avoided or sought after along with many other reasons for taking a detour.

University of British Columbia and their Sailbot team use an occupancy grid approach for planning the path of crossing the Atlantic. The method takes the map and turns it into a grid, occupies the inaccessible space and recursively calculates the fastest route to avoid sailing into different bays and avoiding storms [Team, 2014].

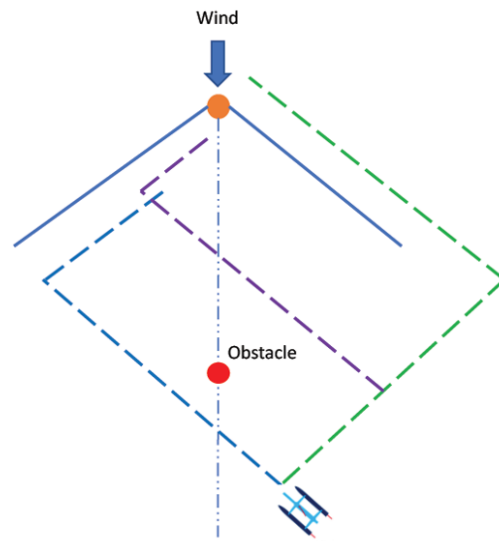


Figure 5.12 Graph of example scenario with the target position located at the top forcing the boat to sail upwind to reach the target position, the different dotted lines are potential paths to be determined by the optimal trajectory control

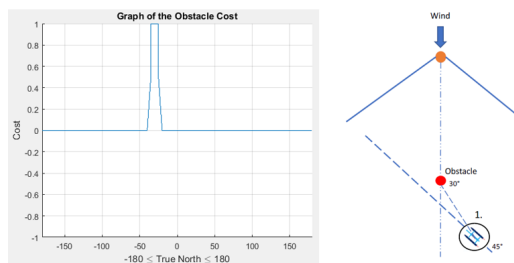


Figure 5.13 Graph of example scenario with the obstacle cost highlighted.

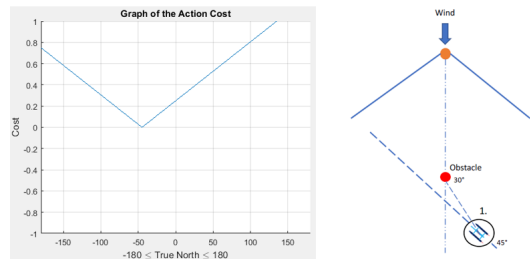


Figure 5.14 Graph of example scenario with the action cost highlighted.

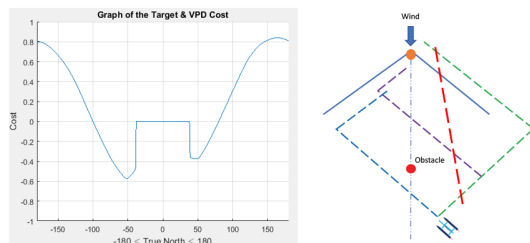


Figure 5.15 Graph of example scenario with the target cost highlighted.

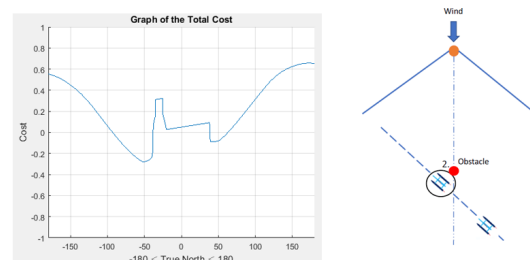


Figure 5.16 Graph of example scenario and the combined total cost assigned to the current situation .

6

Experiments and Simulations

This chapter summarizes the experiments that were carried through. Only a fraction of the different attempts will be brought up as only the most important ones are of essence. The sailing field experiments were conducted at the Robotics Institution in the Software town, Longgang, Shenzhen while the force polar diagram experiments were performed at the RAIL. The main purpose of the experiments were to test the state machine, collect data for modeling and test control approaches. The pool used for sail experiments were determined to be too small to conduct any analysis of the optimal trajectory control and this will be done at the new test site, a lake located near the lab.

6.1 Force Polar Diagram Experiments

The method of bringing forward the FPD is in this section described. The FPD is an important part to the boat dynamics as explained in Chapter 3. To bring these forces and graphs of the forces forward, the setup in Figure 6.1 was used.

As already mentioned in Chapter 3, one common way of modeling the sails are to use the estimation that the sails could be modeled as thin airfoils. In this section one uses the real force created by the wind to model the forces instead of assuming that the force is direct squared proportional to the wind speed. This is solved using Newton's interpolation formula for a 2nd degree polynomial, Equation 6.1 and with the forces being 0 at no wind and the relation squared the $b_0 = 0$, $b_1 = 2$ and $b_2 = 1$.

$$\begin{aligned} y_2 &= b_0 + b_1(x_2 - x_0) + b_2(x_2 - x_0)(x_2 - x_1) \\ \Rightarrow y_2 &= 2(x_2 - x_0) + (x_2 - x_0)(x_2 - x_1) \end{aligned} \tag{6.1}$$

The conclusions drawn are used to model the interstices between the measured force values and these are used for interpolation. There are different measurements



Figure 6.1 The experimental setup of extracting the forces generated by the wind.

that have been collected as of today but more will be collected at a later stage of the research project.

Data Collection

The data was collected through the OPTO force sensor and to measure the wind at an accurate wind speed, the wind speed was also measured with a conventional rotating wind sensor. The force coordinates are shown in Figure 3.5 and show that the x-force is perpendicular to the direction of the sail and the y-force runs along the direction of the sail.

The forces were collected every other degree and a schematic view of the experiments and how the angle representations are structured can be seen in Figure 6.2.

The raw data at the wind speed 2 m/s of the x-force is shown in Figure 6.3 and the y-force is shown in Figure 6.4.

A more intuitive way of displaying how the force correlates with the apparent wind angle is shown in Figure 6.5 and is later used to maximize the forward speed of the boat.

6.2 Test Site Experiments

This section covers a majority of the tests that have been conducted at the test site, it briefly explains each one and discusses the outcome. The test site is mentioned in Chapter 2 and illustrated in Figure 2.3.

A series of tests were performed throughout the project, mainly to ensure that milestones were met. A number of goals were set in parallel with the development

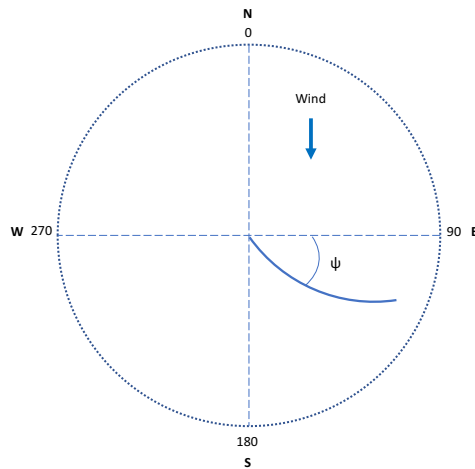


Figure 6.2 The apparent wind angle is ψ and measurements are made at every other angle with the angles 90° to 270° mirrored to the remaining 180°.

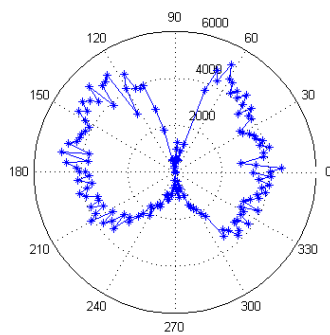


Figure 6.3 The Force Polar Diagram with the F_x force plotted with reference to the apparent wind angle. This is at the wind speed of 2 m/s.

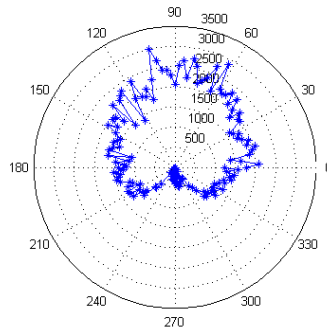


Figure 6.4 The Force Polar Diagram with the F_x force plotted with reference to the apparent wind angle. This is at the wind speed of 2 m/s.

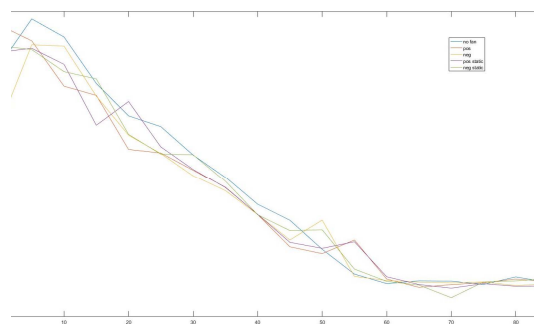


Figure 6.5 The Force Diagram with the y-force plotted with reference to the apparent wind angle. This is at the wind speed of 2 m/s. With different configurations, with $0 \leq \theta \leq 90$

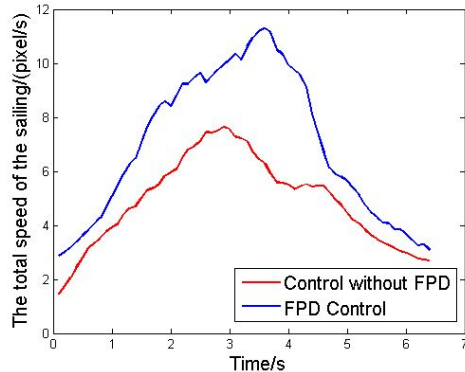


Figure 6.6 Boat speed using the Force Polar Diagram to set the sail angle versus the predefined sail angle.

of the model, controller and optimal trajectory control. Two of these goals were to achieve autonomous tacking and creating a closed loop trajectory, two sets of data later to be used for configuring the model.

Testing Force Polar Diagram Control

As different approaches use different methods to control the sail angle, testing the force polar diagram as a control method was in place. Different tests were conducted, some with the method of controlling the sail angle based on a predefined constant control input and one using the FPD to control what sail angle to choose. Using the Force Polar Diagram to maximize the speed of the boat was proven to be successful, a set of velocities over time can be seen in the graph shown in Figure 6.6.

Model Calibration Tests

To calibrate the model parameters multiple tests were performed, all with the purpose of collecting data later to be used for making sure that the model parameters were describing the boat dynamics. Except for the above mentioned tests, two tests were made especially for the parameter configuration. One test involved sailing with a constant neutral sail and rudder angle and one test was when the rudder angle was set to different values.

Once the data has been collected one can calibrate the model, in this case a weighted least-squares method is to be used as explained in [Hill, 1998]. The weighted least-squares function is shown in Equation 6.2.

$$S(\underline{c}) = \sum_{i=1}^N w_i [y_i - y'_i(\underline{c})]^2 + \sum_{p=1}^{NPR} w_p [P_p - P'_p(\underline{c})]^2 \quad (6.2)$$

Where \underline{c} as the vector of model constants, N as the number of data points collected, w_i as the weight, y_i as the real value, y'_i as the simulated value, NPR as the number of data points before regression, P_p as estimate before regression and p'_p simulated value before regression.

Test Analysis

As for the force polar diagram simulations, a bit of noise was observed. However, as the forces should be the same with reversed sign on the x-force for 180° as for 0° and the same for 179° as for 1° and so on, this means that one can take the mean value for these. The values were also smoothed with a 5 degree moving average filter and linearly interpolated as only every other value was collected.

The purpose of conducting all tests in the pool were that it would be convenient, one would not require another boat for supervision or rescue. As it was already known that the wind would be unstable when considering the standard wind another approach was taken. To try to achieve a constant wind field with constant wind angle and wind speed over the test area it was decided that a 6x10 meter pool with fans at the end would be a better choice than a lake.

The pool did however cause some issues as the fans could not create a constant wind field, the wind intensity was highly irregular as the fans did not reach far down the pool and even between the fans, a distance of 20 centimeter one could observe no wind at all. At the very end of the pool little or no wind could be observed and the wind bounced back along the edges of the pool creating a circular wind flow. It was therefore decided that the model should be further calibrated with the data collected from the new test site.

6.3 Catamaran Simulations

This section further explains the simulations performed with the developed simulation tool. The simulation model is based on multiple interpreted function blocks that together with the control inputs and trajectory control create the tool. The simulink tool developed is shown in Figure 6.7.

The motion of the boat is simulated and continuously plotted and stored to analyze the model constants. Without the improved data from the new test site the empirically determined model constants are set to the values displayed in Table 6.1.

Multiple simulations were executed to test the model, velocities and rotations were observed and the controller was also tested as can be seen in Figure 6.8.

6.4 Heading Control Simulations

As mentioned in Chapter 4, Ziegler-Nichols tuning method was chosen as the approach for tuning the parameters. As the dynamics of the boat is different depending

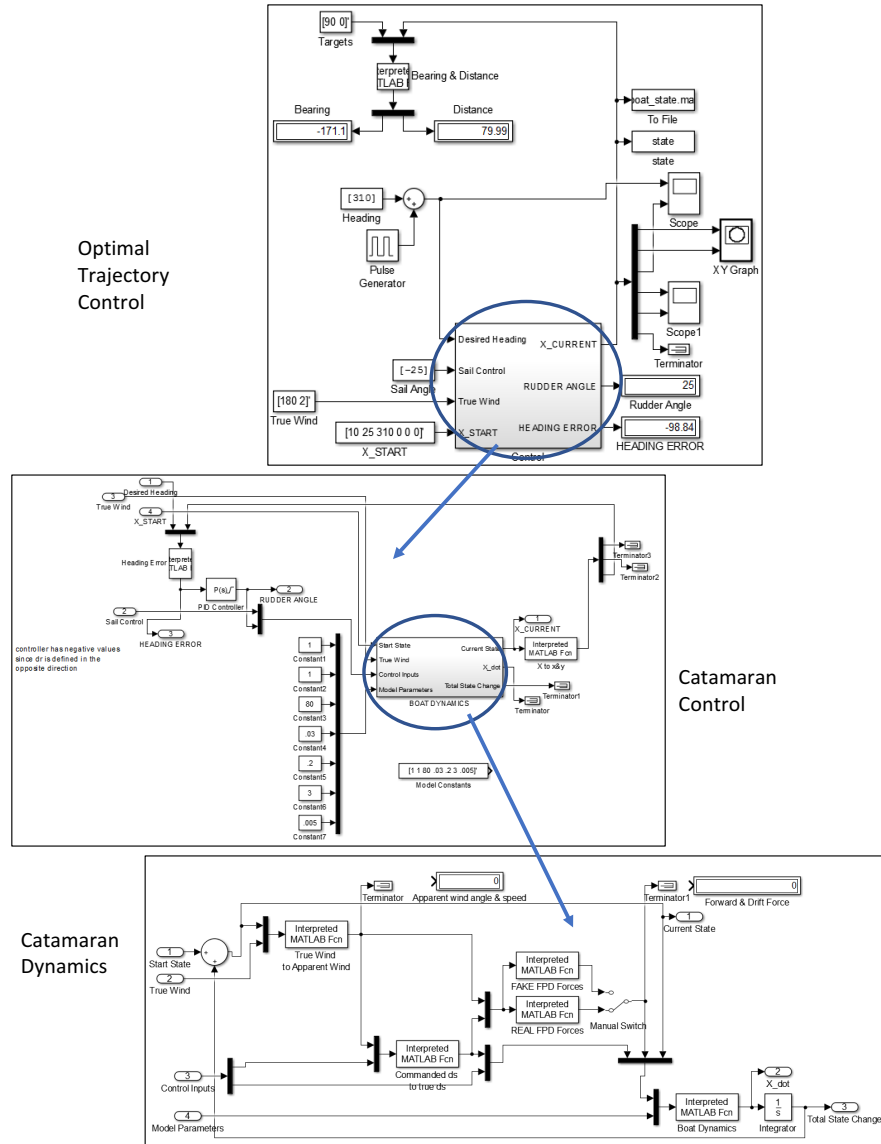


Figure 6.7 This figure show the different relations between the optimal trajectory control level, control and dynamics.

Table 6.1 Experimental Parameters. Parameters determined through tests and simulations.

Parameter	Abbreviation	Value
Forward Decelerating Constant	C_1	1
Rudder Decelerating Constant	C_2	1
Drift Decelerating Constant	C_3	80
Rudder Force Constant	C_6	3
Angular Decelerating Constant	C_7	0.005

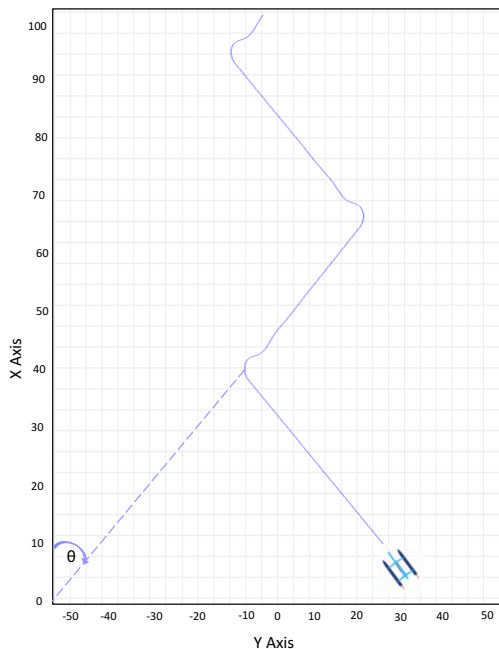


Figure 6.8 Simulation of the boat sailing upwind. the controller receives pulses of desired headings and is controlled thereafter, the wind is going at a $180^\circ \theta$ angle.

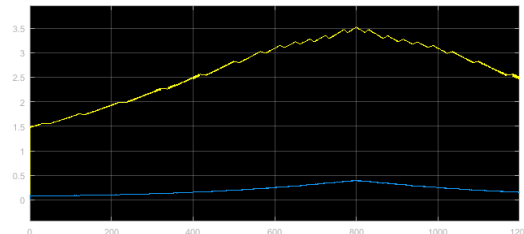


Figure 6.9 Boat speed(yellow) and drift speed(blue) with different simulated sail angles in a ramp function.

on what direction one is sailing with reference to the wind, also these parameters should be altered based on the conditions. For simplicity one may chose control parameters that work without having to alter them based on the boat heading. The chosen parameters are listed in Table 4.1 and the simulations used for tuning them is explained here.

6.5 Sail Control Simulations

To determine the optimal sail angle one can simulate the boat model and find the optimal velocity and what sail angle that result in that velocity. This sail control simulations are strongly correlated with velocity polar diagram and is performed for each heading angle, the simulink tool iterates through all possible sail angles and finds the optimal one. The simulations for sailing at a 90°true wind angle at 2m/s is shown in Figure 6.9. The optimal sail angle can from this simulation be determined and extracted from the figure to be around 3°, small because apparent wind is different from true wind.

7

Conclusions

7.1 Conclusion

During the process of the catamaran development, multiple platforms were used. Initially the controlling hardware was installed on a mono hulled model sailboat, this was discarded because of the depth of the keel which made it difficult to use in the pool test site. Another multi hulled boat was discarded, a trimaran. This was not used because the size of it made it hard to maneuver in the test size, it was too big. As of today the current catamaran works great, another version is to be developed to be more suited for lake sailing.

The model developed seems to capture the dynamics of the boat to a high extent. The parameters could be refitted with the current or new catamaran in the lake were more accurate tests are expected. A model of the boat could be infinitely complex as there are more than the current parameters that affect the motion of the boat, this has been discarded at this stage and with a seemingly good result. Overall the assumption that roll, pitch and heave can be neglected seems correct, as previous research with far more roll neglects these motions also concludes.

The control of the sailboat works well, using the force polar diagram to control the sail angle was proven to improve the motion of the boat, this is especially considering the boat speed which is of essence. When it comes to the rudder controllers, all are being used successfully and the proportional controller controls the boat with little or no oscillations, this does however leave a slight integrating error, an error that is not as important as it might normally be. Even if the boat heading is the same as the desired heading, one can not expect it to sail in the same direction because of the side drag. Therefore using the PID controller can be considered as redundant and PD might be a good approach.

The optimal trajectory control is the part where autonomous sailing can improve the most. The approach proposed is a simple approach that is easy to understand and can be gradually made more complex and improved over time. It can be made infinitely complex same as the model and the features brought forward so far captures the decision making of a sailor to some extent so far.

The test site and experimental setup was continuously improved during the project, starting with a pool with two fans leaving large areas with no wind and a boat that was hard to detect with the cameras mounted. Even with multiple fans, plastic sheets screening off the external real wind and many more fixes, the wind was never perfect. The test site had some flaws as the fans only reached about five meters down the pool, the wind was highly depending on where the boat was located. Even with three fans mounted just at water level one could observe obvious fluctuations in the wind field that was modeled as constant, this complicated the calibration of the software tools.

7.2 Future Work

With regards to the current work some work is yet to be done. As the optimal trajectory control part is in need of some hardware components to detect live obstacles this is to be mounted on the boat. With the fact that the small catamaran is as of now on the heavy side installment of new components will be limited. It is therefore suggested and planned to change to a larger platform to be able to also install GPS and other sensors.

The model parameters need to be re-calibrated using better data with a more constant wind field. Modeling the wind field in the pool with a large wind speed change and even 180°wind direction changes makes the model difficult to tune. Therefore future work will be to collect data and test the boat in a larger area with a more constant wind field.

Both the control and optimal control part becomes affected by model parameters that need perfect tuning and should be re-tuned at a later stage with better parameters.

The research area is interesting and future work is to implement the leanings from this project to the microtransat challenge.

Bibliography

- Arduino Bluno (2017). *Arduino development board*. [Online; accessed April 27, 2017]. URL: <https://www.arduino.cc/en/Main/ArduinoBoardNano>.
- Briere, Y. (2008). “Iboat: an autonomous robot for long-term offshore operation”. *Electrotechnical Conference*.
- Clement, B. (2013). “Control algorithms for a sailboat robot with a sea experiment”. *Conference on Control Applications in Marine Systems*.
- Fossen, T. I. (2002). *Marine Control Systems*. Marine Cybernetics.
- Gale, T. and J. Walls (2000). “Development of a sailing dinghy simulator”. *SIMULATION* 3:74, pp. 167–179.
- Hill, M. C. (1998). *Methods and Guidelines for Effective Model Calibration*. U.S. Department of the Interior.
- I. Giger S. Wismer, S. B.e. a. (2009). “Design and construction of the autonomous sailing vessel avalon”. *Robotic Sailing*, pp. 43–48.
- Jaulin, L. and F. L. Bars (2013). “Sailboat as a windmill”. *Robotic Sailing*, pp. 81–92.
- Jaulin, L. (2012). “A simple controller for line following of sailboats”. In: *Joysway*. Accessed: 2017-04-30.
- Kaiser, M. J. (2011). *Marine Ecology: Processes, Systems and Impacts*.
- M. Tranzatto J. Wirz, e. a. (2015a). “Aeolus, the eth autonomous model sailboat”. *Oceans*.
- M. Tranzatto A. Liniger, S. G.A. L. (2015b). “The debut of aeolus, the autonomous model sailboat of eth zürich”. *Oceans*.
- Nuno A. Cruz, J. C.A.e. a. (2015). “Integration of wind propulsion in an electric asv”. *Robotic Sailing*, pp. 15–27.
- OMD-20-FG-100N DATASHEET (2017). *Opto force sensor*. [Online; accessed April 27, 2017]. URL: <https://optoforce.com/file-contents/OMD-20-FG-100N-DATASHEET-V2.1.pdf?v3>.

Bibliography

- Pêtrès, C., M. Romero-Ramirez, F. Plumet, B. Gas, and S.-H. Ieng (2015). “Toward an autonomous sailing boat”. *IEEE Journal of Oceanic Engineering* **40**:2, pp. 397–407.
- Stelzer, R., T. Pröll, and R. I. John (2007). “Fuzzy logic control system for autonomous sailboats”. *IEEE Fuzzy Systems Conference*.
- Stelzer, R., K. Jafarmandar, H. Hassker, and R. Chawot (2011). “A reactive approach to obstacle avoidance in autonomous sailing”. *The 15th International conference on Advance Robotics*, pp. 20–23.
- Team, U. S. S. (2014). “Beyond the prototype - designing a rout making algorithm”.
- Textor, K. (1995). *The New Book of Sail Trim*. Sheridan House Inc.
- Vaavud Sleipnir (2017). *Vaavud wind sensor*. [Online; accessed April 27, 2017]. URL: https://images.vaavud.com/-K3K4Devz-MP_NWeB00p.
- Xiao, L. and J. Jouffroy (2014). “Modeling and nonlinear heading control of sailing yachts”. *IEEE Journal of Oceanic Engineering* **39**:2, pp. 256–268.

Lund University Department of Automatic Control Box 118 SE-221 00 Lund Sweden		<i>Document name</i> MASTER'S THESIS <i>Date of issue</i> August 2017 <i>Document Number</i> ISRN LUTFD2/TFRT--6038--SE
<i>Author(s)</i> Carl Strömbeck		<i>Supervisor</i> Alex. H. Qian, Robotics and Intelligent Manufacturing Lab The Chinese University of Hong Kong Shenzhen Tore Hägglund, Dept. of Automatic Control, Lund University, Sweden Charlotta Johnsson, Dept. of Automatic Control, Lund University, Sweden (examiner)
<i>Title and subtitle</i> Modeling, Control and Optimal Trajectory Determination for an Autonomous Sailboat		
<i>Abstract</i> <p>A fleet of autonomous sailboat could change our perception of the planet. An autonomous sailboat could not only conduct environmental research but also perform month long operations through the energy efficient wind propulsion. This thesis is the work behind the development of an autonomous catamaran model sailboat.</p> <p>A new mathematical model is brought forward and implemented for simulations performed alongside the proposed control strategy. The model and control strategy is evaluated and empirically verified to work as a subsystem for the optimal trajectory control approach. This method for planning the trajectory of the boat and still avoiding the constraint of the wind is presented as an important step to achieve the end goal of autonomous sailing.</p> <p>The experimental setup performed well, except for some turbulence induced by the wind fans installed to create the artificial wind field at the test site. Both the mathematical model and the controller cause no issues with regards to simulating the motion of the boat. An extended abstract of the paper submitted related to this thesis has been presented successfully at the International Conference on Robotics and Automation 2017 in Singapore.</p>		
<i>Keywords</i>		
<i>Classification system and/or index terms (if any)</i>		
<i>Supplementary bibliographical information</i>		
<i>ISSN and key title</i> 0280-5316		<i>ISBN</i>
<i>Language</i> English	<i>Number of pages</i> 1-74	<i>Recipient's notes</i>
<i>Security classification</i>		